

A large, vertical photograph of a rugged, mountainous landscape in Greenland. The terrain is rocky and sparsely vegetated, with a mix of grey and brown tones. The sky is overcast and grey. The text of the title is centered over the upper half of the image.

**Luminescence dating of sediments
associated with Norse agriculture
from Søndre Igaliku, Greenland**

June 2007

C.I. Burbidge, D.C.W. Sanderson, I.A. Simpson and W.P. Adderley

Summary

This study supports a new investigation into the chronology, and the palaeoenvironmental context and consequences, of Viking settlement in Greenland (section 2). Optically stimulated luminescence (OSL) age determinations have been made for a series of sediments associated with Norse agricultural activity around the farm and church site of Søndre Igaliku, Eastern Settlement (section 3). The geomorphological and archaeological significance of the age determinations has been reviewed in the light of the luminescence results and the samples' depositional contexts, to constrain the deposition/formation dates of the sampled sediments (section 6).

A total of 5 age determinations were made (section 5.3). Dose rate determinations were made using thick source beta counting, high-resolution gamma spectrometry, field gamma spectrometry, measured water contents and calculated cosmic dose rates (sections 4.2.1, 5.1). Equivalent dose determinations were made (sections 4.2.2, 5.2) using the OSL signals from sand sized grains of quartz separated from each sample.

Dose rates ranged from 3.1 to 3.7 mGy/a, D_e values ranged from 2.2 to 3.2 Gy. Age estimates for these samples ranged from 0.66 to 0.94 ka, the average being $0.82 \text{ ka} \pm 0.11$ (section 5.3). Uncertainties on the age estimates were commonly 10 % at one standard error.

The OSL results indicate formation of soils with anthropogenic input from the 11th through into the 14th Centuries AD at Søndre Igaliku, i.e. covering the expected range of Norse settlement in the region (section 6.3). These appear to have subsequently been buried by material dating to the 12th Century, possibly reworked from coastally eroded homefields associated with the same settlement. Consideration of mechanisms for redeposition in the light of the OSL results indicates that the reworking hypothesis should be testable using soil micromorphological analysis of the microbanded layers (6 to 4). Comparison of the OSL results with ¹⁴C results on charcoal from the same sediments indicates that marine reservoir effects and wood-age may combine to produce a residual of c. 100-200 years in calibrated radiocarbon dates (section 6.3).

Contents

Summary	ii
Contents	iii
1. Introduction.....	4
2. Background.....	4
2.1. Context.....	4
2.2. Aims.....	5
2.3. Luminescence dating of sediments	5
3. Sampling	6
4. Methods	9
4.1. Sample preparation	9
4.2. Measurements and determinations.....	9
4.2.1. Dose rate measurements and determinations.....	9
4.2.2. Luminescence measurements.....	11
5. Results.....	12
5.1. Dose rates.....	12
5.2. Single aliquot equivalent dose determinations	15
5.3. Age estimates	17
6. Discussion.....	17
6.1. Equivalent dose.....	17
6.2. Dose rate	19
6.3. Ages	20
7. Conclusions.....	23
References.....	24
Appendix A. Luminescence sampling forms (by Ian Simpson).....	26
Appendix B. Sample preparation and measurement.....	31
Appendix C. Dosimetry	32
C.1. Thick source beta counting	32
C.2. High resolution gamma spectrometry	35
C.3. Field Gamma Spectrometry	40
C.4. Cosmic dose rate	42
C.5. Water content	42
Appendix D. Equivalent dose determinations	43

1. Introduction

This report is concerned with optically stimulated luminescence (OSL) investigations of sediment samples recovered from a sequence of Norse homefield deposits from Søndre Igaliku, Southwest Greenland, 45°16' W, 60°54'N. Samples were taken by Prof. Ian Simpson in summer 2006, from layers in the sequence containing some evidence of anthropogenic input: to date the main phase of anthropogenic soil development and test models of site abandonment and/or sedimentary reworking.

2. Background

2.1. Context

Edwards *et al.*, 2004 outline how the programme “Landscapes circum-Landnam: Viking settlement in the North Atlantic and its human and ecological consequences”, aims to address “what happens environmentally and socially when a group of people colonise ‘pristine’ landscapes, focussing on initial settlement in the Faeroes, Iceland and Greenland”. They describe the main research themes as: “the pre-Landnam resource base”, “Landnam landscapes”, and “sustainable settlement?”, and include radiometric dating of a range of farms and proxy records to test current models of settlement, sustainability, and abandonment.

As part of this programme, soils-based records from Norse homefields in the area of Vatnahverfi (Eastern Settlement) are being examined. Simpson (pers. comm.) describes homefields as managed agricultural areas surrounding Norse farmsteads, which were important for direct subsistence and for fodder production. He selected contrasting sites for examination: Ø70 (small upland farm); Ø71 (large low lying site, with north and south farms); Ø167 (large upland farm); Ø78 (Eqaluít - large low lying Norse farm and church site); Ø196 (low lying small farm), and Søndre Igaliku (Ø66): a large low-lying farm and church site and the subject of the present study.

Radiometric dating of these sites is largely being conducted through ¹⁴C dating of shrub birch (*betula nana*) charcoal. However, Ø66 was interpreted as lying in an area of erosion and deposition, with the possibility of re-working (Simpson, pers comm.). It is also coastally located: determination of ¹⁴C reservoir effects in this region and timeframe forms part of the Landscapes circum-Landnam programme (Edwards *et al.*, 2004).

The recorded sedimentary sequence consists of 11 layers above bedrock, differentiated according to colour and texture (Figure 3.1): layer 1 is the modern topsoil; layers 2 and 3 are sandy wind-blown deposits thought to be relatively recent (modern sub-aerial reworking of sand in the area is illustrated on the title page of this report, picture from Simpson, pers comm.); layers 4 and 5 are sandy loams of indeterminate provenance (archaeological/environmental indications are Norse or later Thule Inuit, sedimentology indicates they may have been redeposited); layer 6 is thought to be Norse period soil accumulated in situ but with relatively low anthropogenic input; layers 7 and 8 are more highly enhanced Norse soil layers, layer 8 is tentatively associated with the initial Landnam period (post-985 AD); layer 9 is

an organic loam that may represent the pre-Landnam land-surface; layers 10 and 11 are mineral sands interpreted as alluvial.

Only the potentially cultural layers (4-8) were sampled. The fine texture and dark colour of the cultural layers is likely to have arisen from the addition of manure and/or midden material, but the soils are relatively thin (c. 10-20 cm) and thus appear to have accumulated more or less gradually. Examination of Figure 3.1 indicates that of these only layer 8 retains no soft-sediment structure: layer 7 retains nodular structure while the remainder exhibit microbanding. Layer 8 may thus have been cultivated but the remainder apparently have not. Microbanding may indicate regular minor episodes of wind blown sand inundation. The sand is sub-aerially transported from a proximal source, possibly coastal (see photo on title page, from Simpson (pers comm.)), but is likely to have been derived in the recent geological past from glacial/periglacial weathering of the local bedrock, which is assumed to be granite.

2.2. Aims

The principal aim of the present study is to support a new investigation into Viking settlement in the North Atlantic. Specifically the present study aims to use OSL to date the deposition of sediments associated with Norse agricultural activity around one Viking settlement in Southern Greenland (Søndre Igaliku), and to examine sedimentary mechanisms that have operated at the site. These results are to be compared with ^{14}C dates for the growth of shrub birch, found as charcoal within the sediments.

2.3. Luminescence dating of sediments

Optically stimulated luminescence originates as a consequence of energy deposited within sedimentary minerals in response to naturally occurring ionising radiation in the sample and its environment. By stimulating the minerals in the laboratory using lasers or other suitable light sources, part of this stored energy is released, resulting in luminescence that can be measured to quantify the radiation history of the sample. Luminescence signals can be erased either by heat or exposure to daylight, and for sedimentary materials exposure to light during erosional or transport phases acts as the zeroing mechanism. Enclosure of the sediment after final deposition protects it from light and allows the accumulation of luminescence signals that can be used for age estimation. The luminescence age is determined by combining luminescence determinations of the radiation dose equivalent to the signals recovered from the samples (the equivalent dose), with measurements of the radiation dosimetry of the sample and its environment (the dose rate). The natural dose rate comprises alpha, beta and gamma radiation produced by the decay of naturally occurring radionuclides (^{40}K , and the U and Th decay series), and cosmic radiation. The luminescence age is the quotient of equivalent dose over dose rate.

With sediment dating it is important to recognise that the luminescence age might represent an accumulated signal originating from many cycles of erosion, transport, bleaching and deposition. Only in the situation where undisturbed sediments are available and associated with effective zeroing at time of deposition can sediment dates be interpreted in terms of simple events. Photostimulation, or optical

stimulation, targets readily reset luminescence signals, and regenerative procedures for determining the stored dose within single aliquots or mineral grains (Murray and Wintle, 2000) provided a means of assessing the homogeneity of doses within sediments. This approach can provide important information for diagnosing mixed sedimentary systems, and hence assists the interpretation of luminescence age determinations (e.g. Olley *et al.*, 1998; 1999). It is also important to recognise that the dose rate values for age estimation are based on contemporary measurements of the sample and its environment. The appropriateness of these determinations is assessed with respect to spatial and temporal variations from the average dose rate to the sample in-situ during its burial. Expected deviations are modelled and used to adjust the measured values, e.g. dose rates in clast rich sediments or thin sedimentary layers may be better represented by certain measurement methods: water absorbs radiation, so average water content during burial is estimated using the sample's water retention properties and by modelling its hydrological history: gross precipitation or leaching of radionuclides can be detected using gamma spectrometry: U series mobilisation and disequilibrium may also require modelling.

It is probable that for the samples in the present study, the coarse hard mineral fraction, used for luminescence measurements, contains mineral grains weathered from bedrock in the recent geological past by glacial action and subjected to limited reworking in an environment with relatively low levels of sunlight intensity. Such materials often have low luminescence sensitivity, and retain substantial geological luminescence in less optically stimutable traps (e.g. Alexanderson, 2007; Rhodes, 2000). Careful preparation and measurement is therefore required to recover an uncontaminated signal that was optically zeroed at deposition. Further, sequences of archaeological soils such as the subject of the present study are likely to contain natural wind blown sand and anthropogenic manure, which may have been mixed by cultivation. If the sand is rapidly redeposited or the manure derived from old midden material, then they may contain residual signals. Cultivation may mix together material deposited at different times (Burbidge, 2003).

The present report outlines the samples collected, the measurements undertaken, and the conclusions that can be drawn from the OSL results.

3. Sampling

Sampling was undertaken in May 2006 by Prof. Ian Simpson. Luminescence sampling forms are attached in Appendix A. Samples were taken from five layers through a phase of cultural deposits associated with Norse agricultural activity Figure 3.1. These deposits sealed a banded layer (9) above layers interpreted as natural alluvial material (10 & 11) overlaying bedrock, and were sealed by sandy wind blown deposits in which charcoal was not observed. Sampling details, including the names assigned to each tube and bulk sample in the field, and the laboratory (SUTL) numbers assigned to each upon arrival at the SUERC luminescence dating laboratories, are summarised in Table 3.1.

Figure 3.1. Map showing location of Søndre Igaliku and other Norse settlements in the region (from Mikkelesen *et al.*, 2001), and Ø66 Søndre Igaliku homefield section with context descriptions (adapted from Simpson, pers comm.).

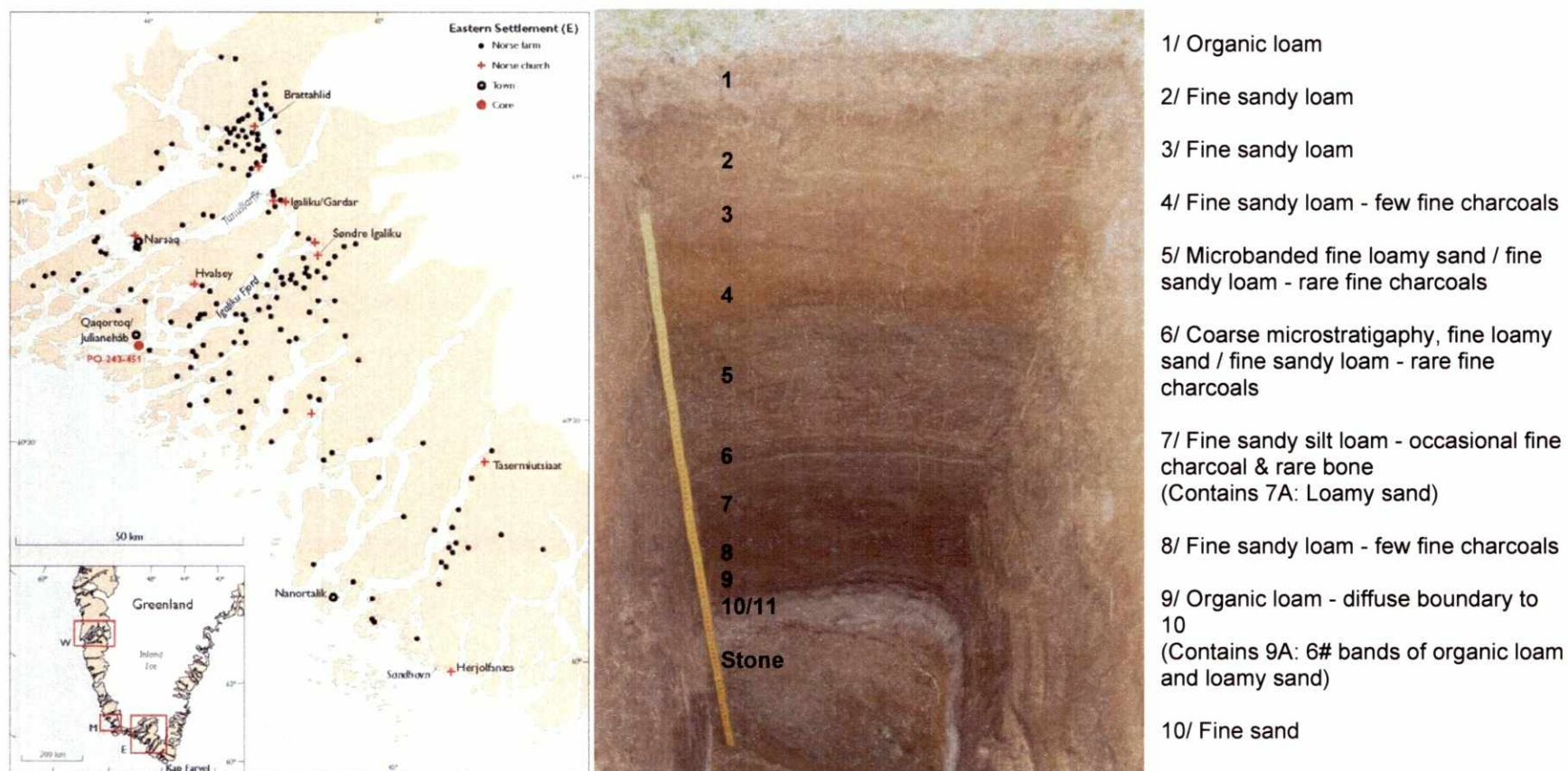


Table 3.1. Sample locations, descriptions, and SUERC laboratory numbers

Sample Number		Type	Mass Dry Sed. (g)	Coordinates		Depth (cm) ^a	Site	No.	Description	Context	
SUERC	Field			N	E					Questions	Questions
SUTL 2085	SI 1	Tube	104	60° 53.529	045° 16.512	40	Søndre Igaliku (Ø66)	4	Fine sandy loam, cultural/redeposited?	Late or Post Norse?	Redeposited Material?
SUTL 2086	SI 2	Tube	104	60° 53.529	045° 16.512	55	Søndre Igaliku (Ø66)	5	Microbanded fine sandy loam, cultural/redeposited?	Norse?	Redeposited Material?
SUTL 2087	SI 3	Tube	100	60° 53.529	045° 16.512	65	Søndre Igaliku (Ø66)	6	Fine sandy loam / loamy sand, Norse, cultural	TAQ balance shifts from cultural to natural input	
SUTL 2088	SI 4	Tube	62	60° 53.529	045° 16.512	73	Søndre Igaliku (Ø66)	7	Fine sandy silt loam, Norse, intense cultural	TAQ major period of soil enhancement	
SUTL 2089	SI 5	Tube	62	60° 53.529	045° 16.512	85	Søndre Igaliku (Ø66)	8	Fine sandy loam, Norse, intense cultural	Initial Landnam?	TAQ soil enhancement

a. values in italics estimated from section diagrams b. TAQ: terminus ante-quem, TPQ: terminus post-quem

4. Methods

4.1. Sample preparation

All sample handling and preparation was conducted under safelight conditions in the SUERC luminescence dating laboratories.

Each sample was first subject to water content determination in the sampling tube. The tubes were unpacked and weighed with gauze taped over one end (“field”). They were then soaked in deionised water for two hours and reweighed (“saturated”), then allowed to drain at room temperature overnight and reweighed (“drained upper limit”), and finally dried at 50°C and reweighed (“dry”). Sample material was then extracted from the tubes: potentially light exposed material from the ends was first removed, then the “core” was excavated for further measurements. Up to ~100 g of the core material was weighed into HDPE pots for high-resolution gamma spectrometry (HRGS) measurement. The pots were sealed with epoxy resin and left for at least 4 weeks prior to measurement to allow equilibration of ²²²Rn daughters. After HRGS measurement the pots were opened and 20 g sub-sampled for thick source beta counting (TSBC) measurement. Following this the core sample material was recombined, and sub-sampled for further processing to obtain a sand-sized quartz separate for equivalent dose determination. Approximately 50 g of bulk material was processed for each sample where available.

With the object of separating sand-sized quartz grains from the bulk sediment, luminescence subsamples were wet sieved to obtain 90-150 µm grains, which were treated with 1 M HCl for 10 minutes to dissolve carbonates: no strong reactions were observed. The treated material was centrifuged in heteropolytungstate solution (LST Fastfloat) at densities of 2.62 and 2.74 g/cm³. The 2.62 - 2.74 g/cm³ fraction was treated with 40% Hydrofluoric acid (HF) for 40 minutes, to dissolve less chemically resistant minerals with a similar density to quartz, and to etch the outer part of the quartz grains, which would have absorbed external alpha radiation during burial. The HF etched material was then treated with 1 M HCl for 10 minutes to dissolve any precipitated fluorides, and re-sieved at 90 µm with ultrasonic agitation to wash off any residual mineral dust. This etched quartz material was dried at 50°C, and dispensed in ~4 mg aliquots onto the central part of 1 cm diameter, 0.25 mm thick stainless steel disks, using silicone oil for adhesion. 16 disks were made per sample.

4.2. Measurements and determinations

4.2.1. Dose rate measurements and determinations

Dose rates were measured in the laboratory using High Resolution Gamma Spectrometry (HRGS) and Thick Source Beta Counting (TSBC). In-situ gamma spectra were measured using a Field Gamma Spectrometer (FGS) by the Prof. Ian Simpson, at the time of sampling.

FGS measurements were made using an Ortec DigiBASE spectrometer pack with a 2”x 2” NaI probe. Prior to fieldwork, measurements were made using this system on the doped concrete reference pads at SUERC in order to provide cross-reference to

dose-rate conversion factors established by Sanderson (1986), based on comparisons with TL dosimetry in doped blocks then at the Oxford and Risø luminescence laboratories. The spectra were calibrated to the 1461 keV peak from ^{40}K and the 2614.5 keV peak from ^{208}Tl , then dose rates were determined from integral counts >450 keV, >1350 keV. Using this approach yielded dose rates from the pads that were on average within 2% and 5% of those expected for the >450 keV and >1350 keV integrals. Field spectra were each measured for 1 hr in holes cut around the luminescence sampling positions using an over-tube, and calibrated to the 1461 keV peak from ^{40}K and the 2614.5 keV peak from ^{208}Tl before calculation of dose rates.

HRGS measurements were performed using a 50% relative efficiency “n” type hyper-pure Ge detector (EG&G Ortec Gamma-X) operated in a low background lead shield with a copper liner. Gamma ray spectra were recorded over the 30 keV to 3 MeV range from each sample, interleaved with background measurements and measurements from Shap Granite in the same geometries. Counting times of 25, 50, and 80 ks per sample were used according to the quantity of material available from each sample. The spectra were analysed to determine count rates from the major line emissions from ^{40}K (1457 keV), and from selected nuclides in the U decay series (^{234}Th , ^{226}Ra + ^{235}U , ^{214}Pb , ^{214}Bi and ^{210}Pb) and the Th decay series (^{228}Ac , ^{212}Pb , ^{208}Tl) and their statistical counting uncertainties. Net rates and activity concentrations for each of these nuclides were determined relative to Shap Granite by weighted combination of the individual lines for each nuclide. The internal consistency of nuclide specific estimates for U and Th decay series nuclides was assessed relative to measurement precision, and weighted combinations used to estimate mean activity concentrations (in Bq kg^{-1}) and elemental concentrations (% K and ppm U, Th) for the parent activity. These data were used to determine infinite matrix dose rates for alpha, beta and gamma radiation.

Beta dose rates were also measured directly using the SUERC TSBC system (Sanderson, 1988). Sample count rates were determined with six replicate 600 s counts for each sample, bracketed by background measurements and sensitivity determinations using the SUERC Shap Granite secondary reference material. Infinite-matrix dose rates were calculated by scaling the net count rates of samples and reference material to the working beta dose rate of the Shap Granite ($6.25 \pm 0.03 \text{ mGy a}^{-1}$). The estimated errors combine counting statistics, observed variance and the uncertainty on the reference value.

“Field”, “saturated”, and “drained upper limit” (DUL; Ratiff *et al.*, 1983) values of water content (section 4.1) were calculated as fractions of dry sediment mass after subtracting the mass of the tube and gauze. An assumed value for the average water content during burial was calculated as the average of the field and DUL water contents. The dose rate estimates were used in combination with the assumed burial water contents, to determine the overall effective dose rates for age estimation.

The cosmic dose rate was estimated as follows. The latitude, altitude and (sediment) depth dependencies of cosmic radiation, relevant to luminescence dating, are described by Prescott and Stephan (1982) and Prescott and Hutton (1988). In the present study, the latitude of each sample was approximated to the nearest degree, and altitude was approximated as 0.0 km for all. Surface cosmic dose rate was estimated

using Prescott and Stephan (1982), Eqn. 1, with latitude dependent parameters read from Fig. 2. A representative value for the average burial depth of each sample since the luminescence signal was last zeroed, was estimated from depth at the time of sampling, geomorphological context, and approximate luminescence age. Depth was converted to mass-depth assuming sediment bulk density to be 1.6 g/cm^3 , and a fit to the dose rate vs. depth data of Prescott and Hutton (1988) was used to calculate the cosmic dose rate at that depth. Uncertainties were calculated as: 5% plus the difference between cosmic dose rate at the depth of sampling, and that at the estimated average burial depth.

4.2.2. Luminescence measurements

All measurements were conducted using a Risø DA-15 automatic reader, equipped with a $^{90}\text{Sr}/^{90}\text{Y}$ β -source for irradiation, blue LEDs emitting around 470 nm and infrared laser diodes emitting around 830 nm for optical stimulation, and a U340 detection filter pack to detect in the region 270-380 nm, while cutting out stimulating light (Bøtter-Jensen *et al.*, 2000).

The discs of quartz grains from the tube samples were subjected to a single aliquot regeneration (SAR) sequence (Murray and Wintle, 2000). According to this procedure, the OSL signal level from an individual disc is calibrated to provide an absorbed dose estimate using an interpolated dose-response curve, constructed by regenerating OSL signals by irradiation in the laboratory. This estimate is termed the equivalent dose (D_e), since it is the laboratory dose producing an equivalent signal to that observed from the natural sample. Sensitivity changes which may occur as a result of readout, irradiation and preheating (to remove unstable radiation-induced signals) are monitored using small test doses after each regenerative dose. Each measurement is standardised to the test dose response determined immediately after its readout, thus compensating for observed changes in sensitivity during the laboratory measurement sequence.

In a SAR sequence then, each disc is subject to a number of measurement cycles: Natural&Test (cycle 1), Regenerative&Test (cycle 2), Regenerative&Test (cycle 3), etc., where all that is varied is the regenerative dose. For the purposes of interpolation, the regenerative doses are chosen to encompass the likely value of the equivalent (natural) dose. A repeat dose point is included to check the ability of the SAR procedure to correct for laboratory-induced sensitivity changes, a zero dose point is included late in the sequence to check for recuperative signals, and a repeat point with infrared stimulation prior to the OSL measurement is included to check for non-quartz signal (“Recycling”, “Zero”, “IRRecycling”; Table 4.1). Quartz responds to blue light but generally not to infrared light, whereas other common minerals such as feldspars and zircon respond to both. Additionally, results may vary with the severity of the preheating employed: this is tested for by applying a range of preheats to different groups within the set of discs.

In the present study 16 discs per sample were measured using 4 discs each at 4 different preheats (Table 4.1). Regenerative doses of 0 to 15 Gy were applied to all samples (plus repeats etc.: cycles 1 to 9, Table 4.1).

Table 4.1. Quartz Single Aliquot Regenerative Sequence

Aliquots	Operation	Measurement Cycle: Details	1	2	3	4	5	6	7	8	9
			Natural	Linear-spaced doses					Zero	Recycling	IR Recycling
1-16	Regenerative Dose	"X" Gy ⁹⁰ Sr/ ⁹⁰ Y	no	6	3	9	12	15	0	6	6
1-4	Preheat	200°C for 30s	yes	yes	yes	yes	yes	yes	yes	yes	yes
4-8	Preheat	220°C for 30s	yes	yes	yes	yes	yes	yes	yes	yes	yes
9-12	Preheat	240°C for 30s	yes	yes	yes	yes	yes	yes	yes	yes	yes
13-16	Preheat	260°C for 30s	yes	yes	yes	yes	yes	yes	yes	yes	yes
1-16	Measurement	IRSL 120s at 50°C	no	no	no	no	no	no	no	no	yes
1-16	Measurement	OSL 60s at 125°C	yes	yes	yes	yes	yes	yes	yes	yes	yes
1-16	Test Dose	"X" Gy ⁹⁰ Sr/ ⁹⁰ Y	3	3	3	3	3	3	3	3	3
1-16	Test Preheat	160°C for 30s	yes	yes	yes	yes	yes	yes	yes	yes	yes
1-16	Test Measurement	OSL 60s at 125°C	yes	yes	yes	yes	yes	yes	yes	yes	yes

5. Results

5.1. Dose rates

HGRS results are shown in Table 5.1, both as activity concentrations (i.e. disintegrations per second per kilogram) and as equivalent parent element concentrations (in % and ppm), based in the case of U and Th on combining nuclide specific data assuming decay series equilibrium. K concentrations ranged from 2.1 to 2.5 %, the mean was $2.3 \% \pm 0.2$. U concentrations ranged from 3.6 to 4.8 ppm, the mean was $4.4 \text{ ppm} \pm 0.8$. Th concentrations ranged from 8.0 to 11.8 ppm, the mean was $10.0 \text{ ppm} \pm 1.6$. The concentration ratio Th/U is also listed in Table 5.1, to indicate the relative contribution of Th and U to the samples' dose rates. Th/U for the present samples ranged from 2.1 to 2.5, with a mean value of 2.3 ± 0.2 .

Infinite matrix alpha, beta and gamma dose rates from HGRS are listed in Table 5.2, with in-situ gamma dose rates from FGS, infinite matrix beta dose rates from TSBC, and the ratio of beta dose rates from TSBC/HGRS. In-situ gamma dose rate (FGS) ranged from 0.94 to 1.10 mGy/a, the mean was $1.01 \text{ mGy/a} \pm 0.06$. Gamma dose rate measured on a dry sample in the laboratory (HGRS) ranged from 1.33 to 1.74 mGy/a, the mean was $1.58 \text{ mGy/a} \pm 0.17$. Beta dose rate from HGRS ranged from 2.51 to 3.09 mGy/a, the mean was $2.87 \text{ mGy/a} \pm 0.24$. Beta dose rate from TSBC ranged from 0.20 to 1.62 mGy/a, the mean was $0.80 \text{ mGy/a} \pm 0.30$. Alpha dose rate (HGRS) ranged from 16 to 22 mGy/a, the mean was $20 \text{ mGy/a} \pm 2$. The ratio of beta dose rates from TSBC and HGRS was consistently 0.93.

Effective dose rates to the HF etched 120 μm quartz grains used for equivalent dose determination in the present study are listed in Table 5.3, with water content measurements and the assumed values used for calculation of effective dose rate. Etching removes the external alpha contribution to the dose rate (so these are not tabulated), and 10 % of the beta dose rate. Cosmic dose rates are as calculated (section 4.2.1), gamma dose rates are corrected for water content, while beta dose rates are corrected for etching and water content.

Field water content, as a fraction of dry sediment mass, ranged from 0.16 to 0.18, the mean was 0.17 ± 0.01 . Saturated water content ranged from 0.29 to 0.45, the mean was 0.34 ± 0.06 . The drained upper limit (DUL) of water content ranged from 0.29 to 0.43, the mean was 0.34 ± 0.06 . The field water contents were assumed to be low

relative to the average the sample experienced during burial, such that the average value was most likely to lie between the measured field and DUL values. Assumed values for average water content during burial were estimated accordingly, and used for age determinations. These ranged from 0.23 to 0.29, the mean was 0.25 ± 0.03 .

The ratio of gamma dose rates from FGS and HGRS, after adjustment for assumed levels of water content, ranged from 0.69 to 0.83, the mean was 0.75 ± 0.05 .

The 25 % difference in gamma dose rate between FGS and HGRS, and the 7 % difference in beta dose rate between TSC and HGRS may both result from differences in the radon retention conditions of each method: whereas the HGRS measurements were conducted with sealed samples that had been stored for radon equilibration, TSBC and FGS measurements were conducted in open geometry and would therefore not be expected to retain full equilibrium radon levels. ~60 % of the beta dose rate and ~98 % of the gamma dose rate from ^{238}U series is produced by post-radon isotopes.

The difference in gamma dose rates could also have been contributed to by differences in water content and measurement geometry from those assumed in the calculation of dose rates. Field gamma dose rate would appear lower if the solid angle of sediment around the FGS probe was less than 4π during measurement and/or the field water content measured from the OSL sample was less than that in the volume "seen" by the FGS probe whilst in situ. To accommodate the range of likely sample conditions during burial, the weighted means of the TSBC and HGRS values, and the FGS and HGRS values, were used for the calculation of effective beta and gamma dose rates to the samples, with "external error" values (e.g. Burbidge *et al.*, 2006).

Effective beta dose rate ranged from 1.9 to 2.3 mGy/a, the mean was $2.15 \text{ mGy/a} \pm 0.17$. Effective gamma dose rate ranged from 0.9 to 1.2 mGy/a, the mean was $1.05 \text{ mGy/a} \pm 0.11$. Effective cosmic dose rate ranged from 0.22 to 0.25 mGy/a, the mean was $0.24 \text{ mGy/a} \pm 0.01$. On average, the beta contribution to overall dose rate was 63 %, the gamma contribution was 31 %, and the cosmic contribution was 7 %.

Table 5.1. Activity and equivalent concentrations of K, U and Th, determined by HRGS

SUTL No.	Activity Concentration			Equivalent Concentration ^{a,b}			
	K (Bq/kg)	U (Bq/kg)	Th (Bq/kg)	K (%)	U (ppm)	Th (ppm)	Th/U
2085	777 ± 20	56.43 ± 2.96	47.00 ± 1.30	2.51 ± 0.06	4.57 ± 0.24	11.59 ± 0.32	2.54 ± 0.15
2086	754 ± 20	59.03 ± 3.13	47.71 ± 1.32	2.44 ± 0.06	4.78 ± 0.25	11.76 ± 0.32	2.46 ± 0.15
2087	655 ± 16	43.78 ± 2.30	32.54 ± 0.62	2.12 ± 0.05	3.55 ± 0.19	8.02 ± 0.15	2.26 ± 0.13
2088	680 ± 16	56.75 ± 2.79	39.00 ± 0.82	2.20 ± 0.05	4.60 ± 0.23	9.61 ± 0.20	2.09 ± 0.11
2089	752 ± 21	54.31 ± 3.16	37.28 ± 1.67	2.43 ± 0.07	4.40 ± 0.26	9.19 ± 0.41	2.09 ± 0.15
Shap	1370 ± 10	148.2 ± 7.4	115.6 ± 1.1	4.43 ± 0.03	12.00 ± 0.06	28.50 ± 0.26	2.38 ± 0.02

a. Conversion factors based on OECD (1994): 40K: 309.3 Bq/kg/%K, 238U: 12.35 Bq/kg/ppmU, 232Th: 4.057 Bq/kg/ppmTh.

b. Shap granite reference, working values based on HRGS relative to CANMET and NBL standards by Sanderson (1986).

Table 5.2. Insitu gamma dose rate measured using FGS, and infinite matrix dose rates determined by HRGS and TSBC in the laboratory.

SUTL No.	FGS, In-Situ ^a		HRGS, Dry ^b		TSBC, Dry ^c		TSBC/HRGS Beta Ratio
	Gamma (mGy/a)	Alpha (mGy/a)	Beta (mGy/a)	Gamma (mGy/a)	Beta (mGy/a)	Beta Ratio	
2085	1.10 ± 0.03	21.26 ± 0.71	3.09 ± 0.06	1.73 ± 0.04	2.87 ± 0.06	0.93 ± 0.03	
2086	1.02 ± 0.03	21.98 ± 0.74	3.06 ± 0.07	1.74 ± 0.04	2.84 ± 0.06	0.93 ± 0.03	
2087	0.94 ± 0.02	15.78 ± 0.53	2.51 ± 0.05	1.33 ± 0.03	2.34 ± 0.05	0.93 ± 0.03	
2088	0.97 ± 0.03	19.87 ± 0.65	2.77 ± 0.05	1.55 ± 0.03	2.58 ± 0.05	0.93 ± 0.03	
2089	1.00 ± 0.02	19.01 ± 0.77	2.92 ± 0.07	1.56 ± 0.04	2.73 ± 0.06	0.93 ± 0.03	

a. Values in italics are interpolated

b. Based on Dose Rate conversion factors from Aitken (1983).

c. Relative to Shap granite reference (Sanderson, 1986).

Table 5.3. Water contents and effective dose rates

SUTL No.	Water Content (frn. dry mass)				Gamma, Assumed WC		Effective Dose Rate (mGy/a)		
	Field	Sat.	DUL	Assumed ^a	FGS (mGy/a)	HGRS (mGy/a)	Beta ^b	Gamma ^c	Cosmic ^d
2085	0.16	0.29	0.29	0.23 ± 0.04	1.03 ± 0.04	1.37 ± 0.07	2.33 ± 0.11	1.14 ± 0.09	0.25 ± 0.04
2086	0.18	0.30	0.29	0.24 ± 0.04	0.95 ± 0.06	1.37 ± 0.06	2.30 ± 0.13	1.17 ± 0.16	0.24 ± 0.04
2087	0.16	0.32	0.31	0.24 ± 0.05	0.87 ± 0.04	1.05 ± 0.06	1.92 ± 0.15	0.93 ± 0.06	0.23 ± 0.04
2088	0.18	0.36	0.37	0.28 ± 0.07	0.87 ± 0.09	1.18 ± 0.09	2.07 ± 0.20	1.03 ± 0.12	0.23 ± 0.04
2089	0.16	0.45	0.43	0.29 ± 0.10	0.87 ± 0.08	1.17 ± 0.12	2.12 ± 0.15	0.96 ± 0.09	0.22 ± 0.04

a. Assumed water content = (Field + DUL)/2 ± |Assumed - Field|/2^{0.5}

b. Calculated using the weighted mean of the effective beta dose rates measured using HRGS and TSBC:
effective beta dose rate = 0.9*infinite beta dose rate/(1+1.25*water content). 0.9 is the average beta attenuation in a 200 micron silicate grain (Mejdahl, 1979).

c. Calculated using the weighted mean of the water content corrected gamma dose rates from HRGS and FGS:
Effective gamma dose rate = gamma dose rate/(1+1.14*WCassumed-WCas-measured).
WCas-measured = Field for FGS, = 0 for HGRS

For the energies found in a typical sedimentary matrix, water absorbs approximately 1.25 times more beta, and 1.14 times more gamma radiation per unit mass than do silicates (Aitken, 1985).

d. Calculated from latitude, altitude, and estimated average depth during burial, using the data of Prescott and Stephan (1982) and Prescott and Hutton (1988).

5.2. Single aliquot equivalent dose determinations

Sample averaged values relating to the aliquots and measurements used for equivalent dose determination are listed in Table 5.4: aliquot-by-aliquot breakdowns can be found in Appendix D.

The average mass of 90 - 150 μm grains on each disk was 3.9 mg, equivalent to c. 1600 grains. The average sensitivity of the OSL signal from these samples to radiation ranged from 7 to 37 cps/mg/Gy, the mean was $19 \text{ cps/mg/Gy} \pm 13$. With repeated SAR measurement cycles, this sensitivity changed to between 1.5 and 1.9 times the starting values, the mean being 1.7 ± 0.1 times. With respect to the internal checks on SAR performance: average recycling ratio for each sample ranged between 0.99 and 1.10, with a mean of 1.05 ± 0.04 , and the effect of IRSL exposure on this ratio was to produce a range of 0.44 to 0.98, with a mean of 0.77 ± 0.20 .

Average zero dose response as a fraction of the recycling dose response ranged from 0.07 to 0.12, the mean was 0.10 ± 0.02 . This indicates residual signals due to accumulated charge transfer during the SAR run equivalent to $0.57 \pm 0.13 \text{ Gy}$. This is a significant fraction of most of the equivalent doses determined in the present study, however zero dose ratios for individual aliquots (App. D) were consistently within errors of zero residual. Constraining growth curve fits to pass through the origin instead of the measured 0 Gy response made little difference to the D_e values obtained, since the majority of equivalent dose values were close to or above the 3 Gy regenerative dose point.

For equivalent dose determination, data from single aliquot regenerative dose measurements were analysed using the Risø Analyst programme, which fitted individual dose response curves and estimated equivalent dose values for each of the 16 disks per sample. A saturating exponential curve was generally fitted to all the measured points except the “IRRecycling” point (section 4.2.2). However, scatter in the data from certain aliquots precluded exponential fitting, and a linear curve was used instead. No consistent patterns of variation in D_e with preheat were apparent (Appendix D). Results from all 16 disks were used in the estimation of central D_e values.

Arithmetic mean D_e values are listed for each sample in Table 5.4, with the “external” uncertainty on the mean value (standard deviation divided by the square root of the number of disks), the standard deviation of the dataset, and “internal uncertainty” on the mean value (errors propagated through the calculation of the mean). The mean D_e values range from 2.8 to 3.8 Gy, the average is $3.4 \text{ Gy} \pm 0.4$. However, examination of the distributions of results from individual aliquots (Appendix D) indicated that some of the mean values were affected by scatter in the data. Since values of D_e were relatively low, and measurement uncertainties were relatively large and variable, a weighted analysis using absolute (rather than proportional) errors was applied to account for statistical variation in the results. To assess levels of underlying scatter in the data, they were analysed in terms of a single normal population with inherent spread (c.f. the weighted mean assumes a single population with no inherent spread). Thus, maximum likelihood estimates of Central D_e , standard error in D_e , and underlying spread (σ) were obtained.

Table 5.4. Equivalent dose determination: samples and results

SUTL No.	Reader	Ali. Mass N (mg) ^a	Sensitivity (cps/mg/Gy) ^a	Sensitivity Change (frn.) ^a	Recycling Ratio ^a	Post IRSL Ratio ^a	Zero Dose Ratio ^a	Mean De ^{a,b,c}				Weighted Central De ^{b,d}				se /σ	Notes ^e
								(Gy)	σ/N ^{1/2}	σ	pe	Type	N	(Gy)	se		
2085	1	16	3.2 ± 0.1	27.6 ± 7.1	1.72 ± 0.16	1.04 ± 0.05	0.98 ± 0.05	0.067 ± 0.012	3.64 ± 0.40	1.61	0.17	LinCAM	16	3.17 ± 0.24	0.81	0.29	>
2086	1	16	4.3 ± 0.2	7.0 ± 0.4	1.79 ± 0.10	0.99 ± 0.05	0.88 ± 0.04	0.099 ± 0.019	3.82 ± 0.51	2.05	0.26	LinCAM	16	3.23 ± 0.29	0.87	0.33	>
2087	1	16	3.5 ± 0.2	12.3 ± 2.8	1.75 ± 0.09	1.02 ± 0.06	0.73 ± 0.11	0.110 ± 0.023	2.84 ± 0.40	1.61	0.24	LinCAM	16	2.33 ± 0.28	0.85	0.32	>
2088	1	32	4.2 ± 0.1	37.4 ± 5.0	1.54 ± 0.05	1.10 ± 0.03	0.44 ± 0.03	0.081 ± 0.006	3.38 ± 1.03	5.80	0.08	LinCAM	30	2.21 ± 0.10	0.51	0.20	=
2089	1	16	4.0 ± 0.2	11.7 ± 1.7	1.93 ± 0.10	1.08 ± 0.06	0.83 ± 0.05	0.119 ± 0.019	3.37 ± 0.24	0.95	0.18	LinCAM	16	3.09 ± 0.22	0.65	0.34	>

a. Values = arithmetic means. Errors = $\sigma/N^{1/2}$, σ = standard deviation, N = number of aliquots

b. Errors incorporate additional 2% source calibration uncertainty

c. pe = propagated error. Propagated through the calculation of the mean from measurement uncertainties for each aliquot

d. LinCAM = "Central Age Model" (e.g. Galbraith *et al.*, 1999) calculated using linear (not logged) data, in this case σ = scatter in the data not explainable by their measurement uncertainties.

e. =/</>: Weighted Central De appears to be representative/an underestimate/an overestimate

5.3. Age estimates

Listed in Table 5.5 are the sums of the effective beta, gamma and cosmic dose rates and the weighted central equivalent dose estimates. Age values were calculated as equivalent dose divided by dose rate, and converted to calendar dates. The precision to which all values are quoted is based on the rounding of associated uncertainties to 1 significant figure.

5 sets of dose rates, equivalent doses, and hence OSL ages were determined. Dose rate ranges from 3.1 to 3.7 mGy/a, the average is 3.4 mGy/a \pm 0.3. De values range from 2.2 to 3.2 Gy, the average is 2.8 Gy \pm 0.5. Age estimates for these samples range from 0.66 to 0.94 ka, with an average of 0.82 ka \pm 0.11. Uncertainties on the age estimates are quoted at 1se. The age uncertainties range from 0.06 to 0.10 ka, the average is 0.08 ka \pm 0.01. These values equate to 8 to 13 % uncertainty, with an average of 10 % \pm 2.

Table 5.5. Dose rates, equivalent doses, ages and calendar dates

Sample Number		Total	Equivalent	Age (ka) ^a	%	Calendar	Notes ^c
SUERC	Field	Dose Rate (mGy/a)	Dose (Gy)				
SUTL 2085	SI 1	3.71 \pm 0.15	3.17 \pm 0.24	0.85 \pm 0.07	8	1150 AD \pm 70	> =
SUTL 2086	SI 2	3.71 \pm 0.21	3.23 \pm 0.29	0.87 \pm 0.09	11	1140 AD \pm 90	> =
SUTL 2087	SI 3	3.08 \pm 0.16	2.33 \pm 0.28	0.75 \pm 0.10	13	1250 AD \pm 100	> <
SUTL 2088	SI 4	3.33 \pm 0.24	2.21 \pm 0.10	0.66 \pm 0.06	8	1340 AD \pm 60	= >
SUTL 2089	SI 5	3.30 \pm 0.18	3.09 \pm 0.22	0.94 \pm 0.08	9	1070 AD \pm 80	> =

a. Ages in ka before 2007 AD b. Errors rounded to 1 significant figure, values rounded accordingly
c. =/</>: equivalent dose / dose rate appears to be representative/an underestimate/an overestimate

6. Discussion

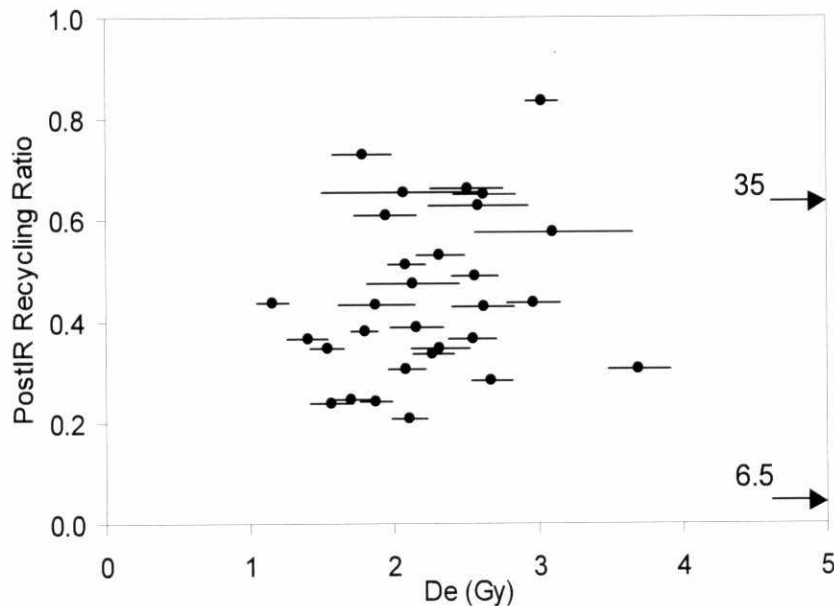
6.1. Equivalent dose

The mineral grains in the Søndre Igaliku sediments are likely to have been eroded from bedrock by glacial action in the recent geological past. Alexanderson (2007) explored the OSL characteristics of recently deposited glaciofluvial quartz from Eastern Greenland. She found 1/ moderate luminescence sensitivity, 2/ low residual signals in sand-sized grains, 3/ thermal transfer of residual signal by harsher preheating during measurement, 4/ relatively poor reproducibility of repeat doses 5/ relatively high infrared responses (but little effect on the absorbed dose values determined). These patterns are consistent with other studies of glacially derived sediment, although larger residual signals and thermal transfer effects have often been observed (e.g. Rhodes, 2000). In this context the luminescence behaviour of the Søndre Igaliku samples may be viewed as relatively benign.

The greater source of age uncertainty arose from scatter in the OSL determinations of equivalent dose, although uncertainty in dose rate was of a similar magnitude. The results from sample SUTL 2088 are central to the archaeological stratigraphy (layer 7) and to issues of uncertainty in equivalent dose. The central De estimate, uncertainty, and underlying spread in the results from sample SUTL 2088 were lower than from the other samples. This could indicate more complete and homogeneous

bleaching of the OSL signal at deposition. This sample also yielded low post IR recycling ratios (average 0.44), indicating that a significant proportion of this signal was sensitive to IR stimulation and therefore unlikely to arise from quartz (section 4.2.2). Optical examination indicated the presence of small and variable numbers of non-quartz grains on the aliquots. However, although post IR recycling ratio (and hence non-quartz signals) varied substantially between aliquots, no trend was evident between post IR recycling ratio and the De value (Figure 6.1).

Figure 6.1. Equivalent dose versus post IRSL ratio for each aliquot measured for SUTL 2088. The two outlying points were excluded from calculation of the central De value for this sample.



OSL investigations and dating in a similar geomorphological context to Søndre Igaliku were conducted by Burbidge (2003) at Old Scatness, Shetland. Gradual accumulation of wind blown sand and organic-rich manure mixed in by cultivation (typical of the Norse soils at Old Scatness), was found to yield De distributions that were often scattered but generally contained a single main grouping. In this case analysis using the weighted central estimate employed in the present study was found to be appropriate and produced OSL dates consistent with archaeological and independent chronometric evidence. Soils rich in redeposited minerogenic midden material yielded more scattered De distributions that could sometimes be resolved, using more complex statistical analysis, into components thought to represent accumulation of the original midden and accumulation of wind blown sand in the soil. A thick (rapidly deposited) layer of windblown sand yielded even more scattered distributions to higher De values, from which a meaningful OSL age for deposition could not be derived.

Examination of the De distributions for each of the Søndre Igaliku samples (Appendix D) indicates that whereas the results from SUTL 2088 exhibit approximately normal scatter with few lower sensitivity aliquots but two extreme outliers (excluded from analyses), the other samples contain more lower sensitivity aliquots that exhibit scatter to high De values. The weighted central estimates are designed to distinguish between genuine scatter and statistical noise, but asymmetric scatter in the

distributions from most samples indicates that the main groupings may have contained some residual signal. This would produce a limited degree of age overestimation such that the true values are likely to lie at the lower end of the allowed uncertainties (Table 5.4). The equivalent dose determinations might be improved by measuring large numbers of smaller aliquots or even single grains and conducting detailed statistical analysis, but it is likely that the relatively low luminescence sensitivities of these samples would limit the precision of such determinations in any case.

6.2. Dose rate

The dose rate uncertainties are limited by uncertainty in past water content and in (past) radionuclide mobility. The main point of interest in the Søndre Igaliku samples is the differences between dose rates measured using different systems (FGS, HRGS, & TSBC, section 4.2.1). It was noted that the differences between the methods may be due to differences in measurement geometry, water content, or radon retention between sealed and unsealed measurements.

If radon were escaping from the samples in-situ but was sealed in for c. 4 weeks prior to the HRGS measurements, there would not have been time for ^{210}Pb to grow back in. Examination of the activity concentrations for each isotope analysed from the ^{238}U series indicates that ^{210}Pb values are similar to or higher than other post-radon isotopes, indicating that Radon loss in the field was not significant. However, there are indications from the relative activity concentrations of ^{234}Th , ^{226}Ra and the post radon isotopes, that ^{238}U has moved from layer 6 (SUTL 2087) to layer 7 (SUTL 2088). The presently measured dose rate for SUTL 2087 may therefore be an underestimate of the average during the sample's burial, and that for SUTL 2088 may be an overestimate (see notes in Table 5.5). These issues could be elucidated through a more detailed radiometric / radiogeochemical investigation of samples from this site.

Table 6.1. Activity concentrations for the isotopes in the ^{238}U series measured using HRGS

SUTL No.	Activity Concentration (Bq/kg)				
	^{234}Th	^{226}Ra	^{214}Pb	^{214}Bi	^{210}Pb
2085	54 ± 3	57 ± 6	56 ± 4	58 ± 3	52 ± 10
2086	60 ± 8	56 ± 6	59 ± 1	59 ± 3	52 ± 11
2087	26 ± 6	30 ± 7	44 ± 2	46 ± 1	63 ± 12
2088	102 ± 9	77 ± 7	53 ± 0.5	52 ± 2	68 ± 11
2089	75 ± 7	63 ± 8	52 ± 1	53 ± 2	71 ± 15
Mean	63 ± 12	57 ± 8	53 ± 3	54 ± 2	61 ± 4

With respect to the other potential factors: The 25 % reduction in field measured gamma dose rate would require water content to be 2.8 times the measured field values, which is 1.4 times the measured values for saturated water content and therefore unable to explain all the difference. Similarly, even if the field probe were placed at the surface of the section pictured in Figure 3.1 there would be no more than around 20% loss in dose rate to the detector unless the stone at the base of the section had very low radioactivity.

However, it should be noted that the 25% lower gamma dose rate from FGS compared to HRGS is equivalent to a difference of 8% in total dose rate, since gamma radiation contributed 31% of the sample's dose rates. Similarly, the 7% higher beta dose rate from TSBC compared to HRGS is equivalent to a difference of 4.5% in total dose rate, since beta radiation contributed 63% of the sample's dose rates. Combining the results to calculate total dose rate (section 5.1) therefore cancels out much of the difference.

6.3. Ages

The above discussion highlights that interpretation of OSL results from sediments such as those from Søndre Igaliku in terms of a simple event chronology is often difficult. However, a series of sediment ages have been measured from Norse cultural layers that are consistent with the expected timeframe of Norse presence in Greenland. Detailed consideration of the equivalent dose and dose rate determinations (above) indicates that:

- 1/ The OSL age for burial of the sediment in the homogenized soil, layer 8 (SUTL 2089) is likely to lie at the younger end of the allowed uncertainties (i.e. Early 12th Century AD). Layer 8 is therefore likely to have developed in the period 990-1150 AD, i.e. since initial settlement c. 985AD.
- 2/ The OSL age of the sediment in the soil layer with nodular inclusions, layer 7 (SUTL 2088) is likely to lie at the older end of the allowed uncertainties (i.e. Late 13th/Early 14th Century AD). Layer 7 is therefore likely to have developed through the 13th Century AD.
- 3/ The OSL age of the sediment in the microbanded cultural layer, layer 6 (SUTL 2087) is likely to lie at the younger end of the allowed uncertainties (i.e. Mid 14th Century AD). Increased scatter to higher values in the equivalent dose distribution from this sample may indicate the inclusion of some older material with incompletely reset OSL signals.
- 4/ The OSL age of the microbanded sediment in layers 4 and 5 (SUTL 2085 and 2086) is likely to lie at the younger end of the allowed uncertainties, i.e. Late 12th Century AD. This material appears older than that in layers 6 and 7 below it, indicating the presence of older material with incompletely reset OSL signals. OSL residuals cannot be large however, since the results do not predate the expected period of Norse settlement in the region.

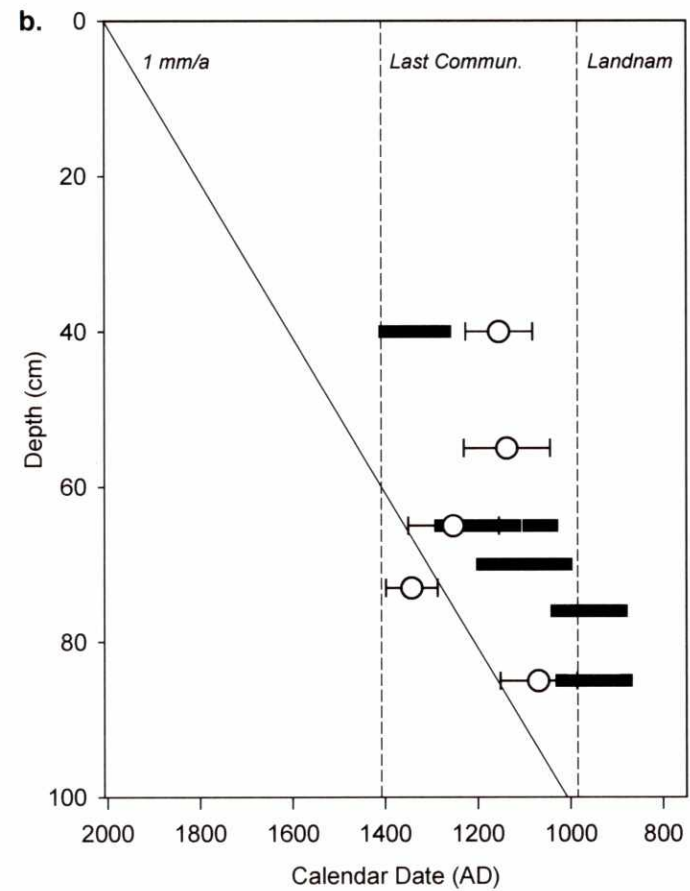
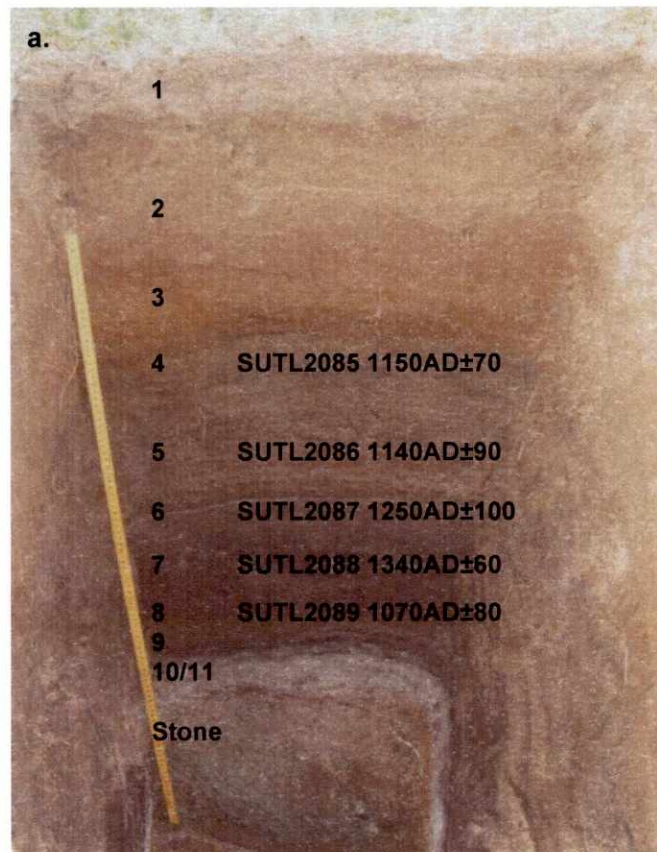
The results from samples SUTL 2087 and 2088 (layers 7 and 8; Figure 6.2) indicate that these layers accumulated through the main period of Norse occupation of the Eastern settlement in Greenland, between c. 985 and 1408 AD (Landnam to last communication from the Eastern Settlement. Edwards *et al.*, 2003; Figure 6.2), with an approximate accumulation rate since initial settlement of c. 0.5 mm/a.

Above layer 7 the sediments exhibit microbanding and the OSL results indicate increased residual signals (Table 3.1; Figure 6.2). Mikkelsen *et al.* (2001) describe a series of banded sediments near Søndre Igaliku and relate the Aeolian component to records of increased storminess around 1300 AD, which were also observed in marine sediments from the adjacent fjord. They also note extensive tidal sediments adjacent to Søndre Igaliku, and evidence for relative sea level rise of c.3 m during the last

c.1000 years in the region, inferring that: “It can therefore not be excluded that this vast area was once fertile lowland utilised by the Norse for production of winter hay for cattle”. The older sediment ages obtained from samples SUTL 2085 and 2086 (layers 4 and 5), and SUTL 2087, indicate that these sediments could indeed have been Norse homeland sediments destabilized by sea level rise and redeposited inland (Table 3.1). In this case the microbanding could have been produced by alternating higher (coarser, cleaner sand) and lower (finer and organic) energy sub-aerial sorting and redeposition. However, in order for the mineral grains to retain much of their luminescence signal, the process of erosion and (sub-aerial) redeposition would have to have been rapid and to have occurred in conditions of low light. Layers 4 to 6 may thus have accumulated quite rapidly.

¹⁴C results on shrub birch charcoal (SUERC 12232-12239), from the same sedimentary section as the OSL samples at Søndre Igaliku, calibrate to Landnam age or older through layer 8 to the lower part of layer 7, then decrease up the section at a rate consistent with c. 1 mm/a sedimentation (Figure 6.2). They do not appear to have been strongly affected by redeposition in the upper layers as inferred from the OSL results. Overall the OSL results are also consistent with an average sedimentation rate around 1 mm/a during the last 1000 years: it is apparent that the rate was lower during the period of Norse occupation and higher later, but additional samples from further up the section would be required to better constrain this. The OSL results from the Norse soils are c. 100-200 years younger than calibrated ¹⁴C, providing an indication of the likely magnitude of marine reservoir offsets and the age of the birch when charred.

Figure 6.2. a. Ø66 Søndre Igaliku homefield section with stratigraphic contexts, SUTL numbers and luminescence results. b. OSL results vs. depth: OSL = circles and $\pm 1\sigma$ errors, ^{14}C = bars covering 95.4% confidence intervals, ^{14}C calibration: Oxcal 3.8, Stuiver *et al.* (1998).



7. Conclusions

The present study supports a new investigation into Viking settlement in Southern Greenland. It has established a sediment-OSL chronology of agricultural activity around the church and farmstead site of Søndre Igaliku. The results indicate formation of soils with anthropogenic input from the 11th through into the 14th Centuries AD, which were subsequently buried by material apparently dating to the 12th Century, possibly reworked from coastally eroded homefields. These results indicate a model for sedimentary accumulation and reworking at this site, which facilitates intercomparison of other chronological, palaeoenvironmental and archaeological data. Hypotheses of reworking in the microbanded layers (6 to 4) should be testable using soil micromorphological analysis.

References

- Adamiec, G., and Aitken, M. J. (1998). Dose-rate conversion factors: update. *Ancient TL* 16, 37-49.
- Aitken, M. J. (1983). Dose rate data in SI units. *PACT* 9, 69-76.
- Aitken, M. J. (1985). "Thermoluminescence dating." Academic Press, London.
- Alexanderson, H. (2007). Residual OSL signals from modern Greenlandic river sediments. *Geochronometria* 26, 1-9.
- Bøtter-Jensen, L., Bulur, E., Duller, G. A. T., and Murray, A. S. (2000). Advances in luminescence instrument systems. *Radiation Measurements* 32, 523-528.
- Burbidge, C. I. (2003). "Luminescence investigations and dating of anthropogenic palaeosols from South Mainland Shetland." Unpublished PhD thesis, Univ. Wales.
- Burbidge, C. I., Duller, G. A. T., and Roberts, H. M. (2006). De determination for young samples using the standardised OSL response of coarse grain quartz. *Radiation Measurements* 41, 278-288.
- Edwards, K. J., Buckland, P. C., Dugmore, A. J., McGovern, T. H., Simpson, I. A., and Sveinbjarnardottir, G. (2004). Landscapes circum-Landnam: Viking settlement in the North Atlantic and its human and ecological consequences - a major new research programme. In "Atlantic Connections and Adaptations." (R. A. Housley, and G. Cole, Eds.). Symposia of the Association for Environmental Archaeology No. 21, Oxbow.
- Galbraith, R. F., Roberts, R. G., Laslett, G. M., Yoshida, H., and Olley, J. M. (1999). Optical dating of single and multiple grains of quartz from jinnium rock shelter, northern Australia, part 1, Experimental design and statistical models. *Archaeometry* 41, 339-364.
- Mejdahl, V. (1979). Thermoluminescence dating: Beta-dose attenuation in quartz grains. *Archaeometry* 21, 61-72.
- Mikkelsen, N., Kuijpers, A., Lassen, S., and Vedel, J. (2001). Marine and terrestrial investigations in the Norse Eastern Settlement, South Greenland. *Geology of Greenland Survey Bulletin* 189, 65-69.
- Murray, A. S., and Wintle, A. G. (2000). Luminescence dating of quartz using an improved single-aliquot regenerative-dose protocol. *Radiation Measurements* 32, 57-73.
- Olley, J., Caitcheon, G., and Murray, A. (1998). The distribution of apparent dose as determined by optically stimulated luminescence in small aliquots of fluvial quartz: Implications for dating young sediments. *Quaternary Science Reviews* 17, 1033-1040.
- Olley, J. M., Caitcheon, G. G., and Roberts, R. G. (1999). The origin of dose distributions in fluvial sediments, and the prospect of dating single grains from fluvial deposits using optically stimulated luminescence. *Radiation Measurements* 30, 207-217.
- Prescott, J. R., and Hutton, J. T. (1988). Cosmic-Ray and Gamma-Ray Dosimetry For Tl and Electron-Spin- Resonance. *Nuclear Tracks and Radiation Measurements* 14, 223-227.
- Prescott, J. R., and Stephan, L. G. (1982). The contribution of cosmic radiation to the environmental dose for thermoluminescent dating. Latitude, altitude and depth dependencies. *PACT* 6, 17-25.

- Ratliff, L. F., Ritchie, J. T., and Cassel, D. K. (1983). Field-Measured Limits of Soil-Water Availability as Related to Laboratory-Measured Properties. *Soil Science Society of America Journal* 47, 770-775.
- Rhodes, E. J. (2000). Observations of thermal transfer OSL signals in glacial quartz. *Radiation Measurements* 32, 595-602.
- Sanderson, D. C. W. (1986). Luminescence Laboratory Internal Report. SURRC.
- Sanderson, D. C. W. (1988). Thick Source Beta-Counting (TSBC) - a Rapid Method for Measuring Beta-Dose-Rates. *Nuclear Tracks and Radiation Measurements* 14, 203-207.
- Simpson, I. (pers comm.). Request for Radiocarbon support: Homefield chronologies at Vatnahverfi, Greenland. University of Stirling, Leverhulme Trust: Landscapes circum Landnám programme.
- Stuiver, M., Reimer, P. J., Bard, E., Beck, J. W., Burr, G. S., Hughen, K. A., Kromer, B., McCormac, G., van der Plicht, J., and Spurk, M. (1998). INTCAL98 Radiocarbon Age Calibration, 24000-0 cal BP. *Radiocarbon* 40, 1041-1083.

Appendix A. Luminescence sampling forms (by Ian Simpson)

Site Code: Ø66 Site Name: Søndre Igaliku		Date: May 2006	Context No: 4	Luminescence Sample No: 1
Description of sampling location :			Sketch of surrounding area	
See attached			See attached	
Photo No:				
Gamma	Reading	Assoc. Sample	Ref No	
Dosimetry				
Details:				
In situ gamma spectrometry from 2 inch NaI detector				
Description of Sample:				
Cultural sediments in Norse homefields, Greenland				
Nature of Dating Problem:				
Date of cultural sediments, evidence of Inuit settlement and comparison with radiocarbon measurement				
Completed By	Checked By	Date		

Site Code: Ø66 Site Name: Søndre Igaliku		Date: May 2006	Context No: 5	Luminescence Sample No: 2
Description of sampling location :			Sketch of surrounding area	
See attached			See attached	
Photo No:				
Gamma	Reading	Assoc. Sample	Ref No	
Dosimetry				
Details:				
In situ gamma spectrometry from 2 inch NaI detector				
Description of Sample:				
Cultural sediments in Norse homefields, Greenland				
Nature of Dating Problem:				
Date of cultural sediments and comparison with radiocarbon measurement				
Completed By	Checked By	Date		

Site Code: Ø66 Site Name: Søndre Igaliku		Date: May 2006	Context No: 6	Luminescence Sample No: 3
Description of sampling location :			Sketch of surrounding area	
See attached			See attached	
			Photo No:	
Gamma	Reading	Assoc. Sample	Ref No	
Dosimetry				
Details:				
In situ gamma spectrometry from 2 inch NaI detector				
Description of Sample:				
Cultural sediments in Norse homefields, Greenland				
Nature of Dating Problem:				
Date of cultural sediments and comparison with radiocarbon measurement				
Completed By	Checked By		Date	

Site Code: Ø66 Site Name: Søndre Igaliku		Date: May 2006	Context No: 7	Luminescence Sample No: 4
Description of sampling location :			Sketch of surrounding area	
See attached			See attached	
Photo No:				
Gamma	Reading	Assoc. Sample	Ref No	
Dosimetry				
Details:				
In situ gamma spectrometry from 2 inch NaI detector				
Description of Sample:				
Cultural sediments in Norse homefields, Greenland				
Nature of Dating Problem:				
Date of cultural sediments and comparison with radiocarbon measurement				
Completed By	Checked By	Date		

Site Code: Ø66 Site Name: Søndre Igaliku		Date: May 2006	Context No: 8	Luminescence Sample No: 5
Description of sampling location :			Sketch of surrounding area	
See attached			See attached	
			Photo No:	
Gamma	Reading	Assoc. Sample	Ref No	
Dosimetry				
Details:				
In situ gamma spectrometry from 2 inch NaI detector				
Description of Sample:				
Cultural sediments in Norse homefields, Greenland				
Nature of Dating Problem:				
Date of cultural sediments and comparison with radiocarbon measurement				
Completed By	Checked By	Date		

Appendix B. Sample preparation and measurement

Sample		Subsample Water Content		For Measurements				Retained unprocessed				For Dosimetry			Date	Date	Date
SUTL	Type	Sample From	Mass Dry Sed (g)	Sample From	Mass (g) Pot	S+P	Sed	Sample From	Mass (g) Pot	S+P	Sed	Sample From	Mass (g)	Pot Type	Gamma Sealed	Gamma Measured	Bctg 20g
2085	Tube	all, in tube	104	core of tube	20.2	119.2	99.0	tube ends	17.6	22.9	5.3	for meas.	99.0	100g wide	150107	220207	280207
2086	Tube	all, in tube	104	core of tube	20.1	118.2	98.1	tube ends	17.2	22.6	5.4	for meas.	98.1	100g wide	150107	210207	280207
2087	Tube	all, in tube	100	core of tube	20.2	116.2	96.0	tube ends	19.0	21.3	2.3	for meas.	96.0	100g wide	150107	260207	290207
2088	Tube	all, in tube	62	core of tube	20.2	76.6	56.4	tube ends	18.0	23.2	5.2	for meas.	50.0	50g	150107	130207	290207
2089	Tube	all, in tube	62	core of tube	19.9	73.7	53.8	tube ends	18.9	26.5	7.6	for meas.	50.0	50g	150107	130207	290207

Sample	Subsample No more prep	Subsample For Lumin	Subsample Mass (g)	Lumin subsample Prep. Settled and Sieved (microns), Retained mass (g)						90-150 micron 10 min 1M HCl				
				Sample From	Mass (g)	Settled	Rinsed	Wet Sieved	date	<90	90-150	150-250	>250"	date
2085	meas. inc dosim.	44.7	meas. inc dosim.	54	6.16	0	180307	not retained	direct to HCl	15.4	3.56	180307	direct to d sep	n
2086	meas. inc dosim.	51.4	meas. inc dosim.	47	4.75	0	180307	not retained	direct to HCl	11.95	4.02	180307	direct to d sep	n
2087	meas. inc dosim.	16.7	meas. inc dosim.	54	7.4	0	180307	not retained	direct to HCl	11.93	7.41	180307	direct to d sep	n
2088	meas. inc dosim.	6.4	meas. inc dosim.	25	5.53	0	180307	not retained	direct to HCl	2.22	3.19	180307	direct to d sep	n
2089	meas. inc dosim.	3.9	meas. inc dosim.	50	13.13	0	180307	not retained	direct to HCl	5.97	3.87	180307	direct to d sep	n

Sample	Lumin subsample Prep. (contd) Density separation (g/cm3)			mass (g) error (g)				2.62-2.74 g/cm3 40min 40% HF, HCl & Resieve				Disks				Measurement			
	Retained (g)	For D. Sep. (g)	date	<2.62 (g) inc pot	2.62-2.74 (g) inc pot	>2.74 (g) inc pot	1.105	0.004	Retained (g) inc pot	Split for HF (g) inc pot	HF <90 (g) inc pot	HF >90 (g) inc pot	Set 1 date	Set 1 No.	Set 2 date	Set 2 No.	Set 1 date	Set 1 file	Set 2 date
2085	6.33	direct to d sep	180307	1.561	direct to HF	1.295	190307	-	direct to HF	1.116	1.377	210307	16	300307	16	210307	stl2r1e	300307	stl3r1h
2086	4.36	direct to d sep	180307	1.493	direct to HF	1.294	190307	-	direct to HF	1.113	1.272	210307	16	300307	16	210307	stl2r1e	300307	stl3r1h
2087	3.78	direct to d sep	180307	1.434	direct to HF	1.37	190307	-	direct to HF	1.121	1.319	210307	16			250307	stl1r1f		
2088	0.69	direct to d sep	180307	1.503	direct to HF	1.342	190307	-	direct to HF	1.13	1.309	210307	16			290307	stl1r1g	100507	stl1r1j
2089	3.11	direct to d sep	180307	1.499	direct to HF	1.387	190307	-	direct to HF	1.129	1.258	210307	16			300307	stl3r1h		

Appendix C. Dosimetry

C.1. Thick source beta counting

Run	940	File	280207	Date	280207		
HV	6.60			Threshold	0.45		
Sample	2085			Mass (g)	20		
	Observed		Rolling Average				
Standard (cps)	3.470 +/- 0.054		3.450 +/-	0.023			
Background (cps)	0.793 +/- 0.015		0.747 +/-	0.004			
Sensitivity (mGy/a/cps)			2.310 +/-	0.030			
Sample	counts	1366	1332	1372	1386	1361	1336
	time	600	600	600	600	600	600
	cps	2.277	2.220	2.287	2.310	2.268	2.227
Mean gross rate (cps)	2.265 +/- 0.014		(SD/rtN) 0.025		(poisson error)		
	cps (false if value > 3SD different from mean)	2.277	2.220	2.287	2.310	2.268	2.227
Mean gross rate (cps)	2.265 +/- 0.014		(SD/rtN) 0.025		(poisson error)		
Net rate (cps)	1.518 +/- 0.025		(poisson error)				
Beta dose rate (Gy/ka)	3.507 +/- 0.075						
Run	941	File	280207	Date	280207		
HV	6.60			Threshold	0.45		
Sample	2086			Mass (g)	20		
	Observed		Rolling Average				
Standard (cps)	3.470 +/- 0.054		3.450 +/-	0.023			
Background (cps)	0.793 +/- 0.015		0.747 +/-	0.004			
Sensitivity (mGy/a/cps)			2.310 +/-	0.030			
Sample	counts	1387	1473	1341	1397	1386	1342
	time	600	600	600	600	600	600
	cps	2.312	2.455	2.235	2.328	2.310	2.237
Mean gross rate (cps)	2.313 +/- 0.033		(SD/rtN) 0.025		(poisson error)		
	cps (false if value > 3SD different from mean)	2.312	FALSE	2.235	2.328	2.310	2.237
Mean gross rate (cps)	2.284 +/- 0.020		(SD/rtN) 0.028		(poisson error)		
Net rate (cps)	1.538 +/- 0.028		(poisson error)				
Beta dose rate (Gy/ka)	3.552 +/- 0.079						

Run	942	File	290207	Date	290207		
HV	6.60			Threshold	0.45		
Sample	2088			Mass (g)	20		
	Observed		Rolling Average				
Standard (cps)	3.414 +/- 0.056		3.445 +/-	0.021			
Background (cps)	0.788 +/- 0.016		0.749 +/-	0.004			
Sensitivity (mGy/a/cps)			2.316 +/-	0.030			
Sample	counts	1377	1331	1352	1354	1329	1354
	time	600	600	600	600	600	600
	cps	2.295	2.218	2.253	2.257	2.215	2.257
Mean gross rate (cps)	2.249 +/- 0.012		(SD/rtN) 0.025	(poisson error)			
	cps (false if value > 3SD different from mean)	2.295	2.218	2.253	2.257	2.215	2.257
Mean gross rate (cps)	2.249 +/- 0.012		(SD/rtN) 0.025	(poisson error)			
Net rate (cps)	1.501 +/- 0.025		(poisson error)				
Beta dose rate (Gy/ka)	3.475 +/- 0.073						
Run	943	File	290207	Date	290207		
HV	6.60			Threshold	0.45		
Sample	2087			Mass (g)	20		
	Observed		Rolling Average				
Standard (cps)	3.414 +/- 0.056		3.445 +/-	0.021			
Background (cps)	0.788 +/- 0.016		0.749 +/-	0.004			
Sensitivity (mGy/a/cps)			2.316 +/-	0.030			
Sample	counts	1268	1271	1163	1225	1267	1216
	time	600	600	600	600	600	600
	cps	2.113	2.118	1.938	2.042	2.112	2.027
Mean gross rate (cps)	2.058 +/- 0.029		(SD/rtN) 0.024	(poisson error)			
	cps (false if value > 3SD different from mean)	2.113	2.118	1.938	2.042	2.112	2.027
Mean gross rate (cps)	2.058 +/- 0.029		(SD/rtN) 0.024	(poisson error)			
Net rate (cps)	1.310 +/- 0.024		(poisson error)				
Beta dose rate (Gy/ka)	3.033 +/- 0.068						

Run	944	File	290207	Date	290207		
HV	6.60			Threshold	0.45		
Sample	2089			Mass (g)	20		
	Observed		Rolling Average				
Standard (cps)	3.414 +/- 0.056		3.445 +/-	0.021			
Background (cps)	0.788 +/- 0.016		0.749 +/-	0.004			
Sensitivity (mGy/a/cps)			2.316 +/-	0.030			
Sample	counts	1342	1338	1359	1356	1373	1434
	time	600	600	600	600	600	600
	cps	2.237	2.230	2.265	2.260	2.288	2.390
Mean gross rate (cps)	2.278 +/- 0.024		(SD/rtN) 0.025		(poisson error)		
	cps (false if value > 3SD different from mean)	2.237	2.230	2.265	2.260	2.288	FALSE
Mean gross rate (cps)	2.256 +/- 0.010		(SD/rtN) 0.027		(poisson error)		
Net rate (cps)	1.507 +/- 0.028		(poisson error)				
Beta dose rate (Gy/ka)	3.491 +/- 0.078						

Run	945	File	290207	Date	290207		
HV	6.60			Threshold	0.45		
Sample	2090			Mass (g)	20		
	Observed		Rolling Average				
Standard (cps)	3.414 +/- 0.056		3.445 +/-	0.021			
Background (cps)	0.788 +/- 0.016		0.749 +/-	0.004			
Sensitivity (mGy/a/cps)			2.316 +/-	0.030			
Sample	counts	1030	993	1024	1011	985	1015
	time	600	600	600	600	600	600
	cps	1.717	1.655	1.707	1.685	1.642	1.692
Mean gross rate (cps)	1.683 +/- 0.012		(SD/rtN) 0.022		(poisson error)		
	cps (false if value > 3SD different from mean)	1.717	1.655	1.707	1.685	1.642	1.692
Mean gross rate (cps)	1.683 +/- 0.012		(SD/rtN) 0.022		(poisson error)		
Net rate (cps)	0.934 +/- 0.022		(poisson error)				
Beta dose rate (Gy/ka)	2.163 +/- 0.058						

Detector	3												
Sample	2086												
Filename	2086												
Roi file	g3aug05.roi												
Date	210207												
Time (ks)	50.00												
Mass (g)	98.1												
	Counts	error	Rate	error	Net Rate	error	Specific Activity	error	Concentration	Within	WM calcs		
			(cts/ks)		(cts/ks)		(Bq/kg)		error	2 err of	WM ?		
40-K	3562	63	71.24	1.26	63.54	1.27	754	20	2.44	0.06			
238-U	238U ppm eU error x/sigm: 1/sigm sum												
234-Th	2452	79	49.04	1.58	12.63	1.62	77	11	6.22	0.89	TRUE	0.64	0.01 full ##### 0.32
	2783	72	55.66	1.44	12.31	1.48	53	7	4.27	0.57	TRUE	1.07	0.02 preRt 3.06 0.05
226-Ra (23	1758	67	35.16	1.34	14.07	1.37	56	6	4.56	0.52	TRUE	1.35	0.02 postF ##### 0.27
214-Pb													
	1154	46	23.08	0.92	20.79	0.93	58	4	4.70	0.34	TRUE	3.27	0.06
	2596	62	51.92	1.24	47.38	1.25	60	4	4.90	0.29	TRUE	4.74	0.08
214-Bi	2144	58	42.88	1.16	38.16	1.18	59	4	4.78	0.30	TRUE	4.44	0.08
	415	37	8.30	0.74	7.74	0.76	55	7	4.48	0.55	TRUE	1.20	0.02
	175	33	3.50	0.66	3.13	0.67	74	19	5.97	1.56	TRUE	0.20	0.00
	431	25	8.62	0.50	6.72	0.51	68	7	5.47	0.56	TRUE	1.43	0.02
	67	25	1.34	0.50	0.75	0.51	26	18	2.10	1.48	TRUE	0.08	0.00
210-Pb	386	35	7.72	0.70	3.84	0.72	52	11	4.23	0.87	TRUE	0.45	0.01
232-Th	232Th ppm eTh error sum												
228-Ac	768	49	15.36	0.98	14.66	1.00	46	4	11.37	0.91	TRUE	3.39	0.07 full ##### 0.76
	1023	46	20.46	0.92	18.13	0.94	53	3	13.06	0.81	TRUE	4.87	0.09
	905	68	18.10	1.36	11.41	1.40	41	5	10.16	1.34	TRUE	1.39	0.03
224-Ra													
212-Pb	5116	130	#####	2.60	88.36	2.66	47	2	11.57	0.41	TRUE	16.79	0.36
212-Bi	272	43	5.44	0.86	4.16	0.88	49	12	12.01	2.86	TRUE	0.36	0.01
208-Tl	106	58	2.12	1.16	0.78	1.19	17	26	4.07	6.31	TRUE	0.03	0.00
	1262	49	25.24	0.98	21.73	1.00	49	3	12.02	0.66	TRUE	6.90	0.14
	154	30	3.08	0.60	2.81	0.62	58	15	14.29	3.68	TRUE	0.26	0.00
	615	27	12.30	0.54	7.30	0.55	47	5	11.62	1.13	TRUE	2.23	0.05
Sample	Specific Activi Concentration Dose Rates (mGy/a)												
			(Bq/kg)		(% or ppm)		Alpha	error	Beta	error	Gamm	error	
Full Series	K	754	20	2.44	0.06				2.02	0.0535	0.587	0.02	
WM	U	59.03	3.128	4.78	0.25	13.28	0.70	0.70	0.037	0.549	0.03		
	Th	47.71	1.317	11.76	0.32	8.69	0.24	0.34	0.0093	0.604	0.02		
	Total	21.98	0.74	3.06	0.0657	1.741	0.04						
Thfull/Ufull	2.46												
Pre 222Rn	U	58.21	19.03	4.714	1.54	13.10	4.28	0.69	0.2252	0.542	0.18		
Post 222Rn	U	59.19	3.743	4.793	0.30	13.32	0.84	0.70	0.0443	0.551	0.03		
Difference		-0.98	19.40	-0.08	1.57	-0.22	4.37	-0.01	0.23	-0.01	0.18		

Detector 2 Sample 2088 Filename 2088 Roi file g2oct06.roi Date 130207 Time (ks) 80.00 Mass (g) 50														
	Counts	error	Rate (cts/ks)	error	Net Rate (cts/ks)	error	Specific Activity (Bq/kg)	error	Concentration error	Within 2 err of WM ?	WM calcs			
40-K	4083		71	51.04	0.89	44.74	0.90	680	16	2.20	0.05			
238-U								238U	ppm eU	error		x/sigma^2 1/sigma' sum		
234-Th	2548		77	31.85	0.96	11.35	1.00	116	12	9.39	0.98	FALSE	0.80	0.01 full 20.35 0.36
	2676		81	33.45	1.01	10.50	1.06	91	10	7.37	0.84	FALSE	0.84	0.01 preRn 3.15 0.04
226-Ra (23	2446		77	30.58	0.96	13.25	1.00	77	7	6.24	0.58	FALSE	1.51	0.02 postRr 17.20 0.32
214-Pb														
	973		49	12.16	0.61	10.62	0.63	53	4	4.26	0.34	TRUE	2.98	0.06
	2500		67	31.25	0.84	27.27	0.86	54	3	4.37	0.26	TRUE	5.15	0.10
214-Bi	2366		65	29.58	0.81	25.34	0.83	55	3	4.48	0.27	TRUE	4.89	0.09
	471		40	5.89	0.50	5.04	0.52	47	6	3.83	0.45	TRUE	1.53	0.03
	207		38	2.59	0.48	2.29	0.49	61	14	4.91	1.14	TRUE	0.31	0.01
	488		33	6.10	0.41	4.40	0.43	50	6	4.08	0.46	TRUE	1.57	0.03
	107		19	1.34	0.24	0.75	0.25	40	14	3.27	1.10	TRUE	0.22	0.01
210-Pb	1024		71	12.80	0.89	6.18	0.92	68	11	5.51	0.89	TRUE	0.56	0.01
232-Th								232Th	ppm eTh	error			sum	
228-Ac	370		38	4.63	0.48	4.10	0.49	38	5	9.38	1.18	TRUE	1.67	0.04 full 47.29 1.21
	1030		54	12.88	0.68	10.52	0.70	43	3	10.64	0.75	TRUE	4.70	0.11
	752		71	9.40	0.89	6.05	0.93	31	5	7.74	1.21	TRUE	1.31	0.04
224-Ra														
212-Pb	5782		134	72.28	1.68	63.05	1.74	39	1	9.70	0.29	TRUE	27.99	0.71
212-Bi	190		40	2.38	0.50	1.72	0.52	27	8	6.61	2.04	TRUE	0.39	0.01
208-Tl	130		46	1.63	0.58	1.04	0.60	34	20	8.31	4.89	TRUE	0.09	0.00
	1289		59	16.11	0.74	13.11	0.76	37	2	9.00	0.55	TRUE	7.36	0.20
	94		30	1.18	0.38	0.89	0.39	27	12	6.69	3.00	TRUE	0.18	0.01
	791		31	9.89	0.39	5.67	0.40	44	4	10.94	0.87	TRUE	3.59	0.08
Sample								Specific Activi	Concentration	Dose Rates (mGy/a)				
Full Series			K	680	16	2.20	0.05			Alpha error	Beta error	Gamma error		
WM			U	56.75	2.788	4.596	0.23	12.77	0.63	0.67	0.033	0.52804	0.03	
			Th	39	0.825	9.612	0.20	7.10	0.15	0.27	0.0058	0.49408	0.01	
			Total					19.87	0.65	2.77	0.0539	1.5517	0.03	
Thfull/Ufull				2.09										
Pre 222Rn			U	88.13	27.99	7.137	2.27	19.84	6.30	1.04	0.3311	0.8201	0.26	
Post 222Rn			U	53.27	3.097	4.314	0.25	11.99	0.70	0.63	0.0366	0.49573	0.03	
Difference				34.86	28.16	2.82	2.28	7.85	6.34	0.41	0.33	0.32	0.26	

Detector		3		Sample		2089		Filename		2089		Roi file		g3aug05.roi		Date		130207		Time (ks)		80.00		Mass (g)		50	
	Counts	error	Rate (cts/ks)	error	Net Rate (cts/ks)	error	Specific Activity (Bq/kg)	error	Concentration error	Within 2 err of WM ?	WM calcs																
							K	%K																			
40-K	3414	63	42.68	0.79	34.97	0.80	752	21	2.43	0.07																	
238-U							238U	ppm eU error		x/sigma^2 1/sigma' sum																	
234-Th	3348	88	41.85	1.10	5.44	1.16	62	14	5.02	1.10	TRUE	0.33	0.01	full	17.21	0.32											
	4251	85	53.14	1.06	9.78	1.12	83	10	6.70	0.84	FALSE	0.76	0.01	preRn	2.20	0.03											
226-Ra (23	2440	76	30.50	0.95	9.41	1.00	63	8	5.08	0.61	TRUE	1.10	0.02	postRr	15.02	0.28											
214-Pb	1044	48	13.05	0.60	10.76	0.62	50	4	4.03	0.32	TRUE	3.12	0.06														
	2326	63	29.08	0.79	24.53	0.81	53	3	4.30	0.27	TRUE	4.91	0.09														
214-Bi	1948	60	24.35	0.75	19.63	0.78	54	4	4.36	0.29	TRUE	4.25	0.08														
	465	42	5.81	0.53	5.25	0.55	62	8	4.98	0.63	TRUE	1.02	0.02														
	136	36	1.70	0.45	1.33	0.47	48	18	3.89	1.47	TRUE	0.15	0.00														
	385	27	4.81	0.34	2.91	0.35	46	6	3.73	0.51	TRUE	1.17	0.03														
	122	27	1.53	0.34	0.93	0.36	79	34	6.43	2.74	TRUE	0.07	0.00														
210-Pb	526	40	6.58	0.50	2.70	0.52	71	15	5.73	1.21	TRUE	0.32	0.00														
232-Th							232Th	ppm eTh error		sum																	
228-Ac	608	55	7.60	0.69	6.90	0.72	44	5	10.84	1.24	TRUE	1.73	0.04	full	22.33	0.60											
	669	46	8.36	0.58	6.03	0.60	34	4	8.27	0.87	TRUE	2.67	0.08														
	979	77	12.24	0.96	5.55	1.01	45	9	11.07	2.11	TRUE	0.61	0.01														
224-Ra																											
212-Pb	4435	139	55.44	1.74	41.47	1.82	39	2	9.60	0.46	TRUE	11.30	0.29														
212-Bi	249	49	3.11	0.61	1.84	0.64	38	14	9.43	3.45	TRUE	0.20	0.01														
208-Tl	198	66	2.48	0.83	1.13	0.87	32	25	7.89	6.21	TRUE	0.05	0.00														
	961	51	12.01	0.64	8.50	0.66	35	3	8.55	0.71	TRUE	4.19	0.12														
	33	34	0.41	0.43	0.15	0.45	5	16	1.25	3.84	FALSE	0.02	0.00														
	635	28	7.94	0.35	2.94	0.37	35	5	8.61	1.17	TRUE	1.56	0.04														
Sample							Specific Activi	Concentration		Dose Rates (mGy/a)																	
							(Bq/kg)	(% or ppm)		Alpha	Beta	Gamma															
Full Series							K	752	21	2.43	0.07	2.02	0.0565	0.5859	0.02												
WM							U	54.31	3.155	4.399	0.26	12.22	0.71	0.64	0.0373	0.50541	0.03										
							Th	37.28	1.669	9.188	0.41	6.79	0.30	0.26	0.0118	0.47224	0.02										
							Total			19.01	0.77	2.92	0.0687	1.56354	0.04												
Thfull/Ufull																											
Pre 222Rn	U	68.30	31.07	5.531	2.52	15.37	6.99	0.81	0.3677	0.63552	0.29																
Post 222Rn	U	52.73	3.512	4.271	0.28	11.87	0.79	0.62	0.0416	0.4907	0.03																
Difference		15.56	31.27	1.26	2.53	3.50	7.04	0.18	0.37	0.14	0.29																

C.3. Field Gamma Spectrometry

Field File Name	Lab File name
Greenland_osl_tube1.spc	e:\rainbow\green1.chn
Greenland_osl_tube3.spc	e:\rainbow\green2.chn
Greenland_osl_tube5.spc	e:\rainbow\green3.chn

```

File      :      e:\rainbow\green1.chn
Live     time      (s)      3595
Energy   calibration coefficients
          b1=      -28.11947
          b2=       2.992208
          b3=         0
E        =          450 keV   in      Ch      159
Integrated counts, count rates (cps)
Total    spectrum :      1357853  377.706
E>450   keV      :      207114  57.61168
E>1350  keV      :      36455  10.14047
Energy   integral :      3.72E+08 keV
Energy   deposition rate :      103437.7 keV/s
Mean     energy   per photon detected :      273.8578
Dose     Rate     (mGy/a) - >450      1.123428  5.77E-02
Dose     Rate     (mGy/a) - >1350      1.07996  5.10E-02
Dose     rate     (mGy/a) - energy      1.586735  7.96E-02

```

```

File      :      e:\rainbow\green2.chn
Live     time      (s)      3595.64
Energy   calibration coefficients
          b1=      -31.66928
          b2=       3.023622
          b3=         0
E        =          450 keV   in      Ch      159
Integrated counts, count rates (cps)
Total    spectrum :      1184678  329.4763
E>450   keV      :      177520  49.37091
E>1350  keV      :      31160  8.666051
Energy   integral :      3.17E+08 keV
Energy   deposition rate :      88297.86 keV/s
Mean     energy   per photon detected :      267.9946
Dose     Rate     (mGy/a) - >450      0.962733  4.94E-02
Dose     Rate     (mGy/a) - >1350      0.922934  4.36E-02
Dose     rate     (mGy/a) - energy      1.354489  6.80E-02

```

File	:	e:\rainbow\green3.chn			
Live	time	(s)	3595.62		
Energy	calibration	coefficients			
	b1=		-17		
	b2=		3		
	b3=		0		
E	=	450 keV	in	Ch	155
Integrated	counts,	count	rates	(cps)	
Total	spectrum	:	1184973	329.5601	
E>450	keV	:	190580	53.00337	
E>1350	keV	:	32772	9.114422	
Energy	integral	:	3.40E+08	keV	
Energy	deposition	rate	:	94445.07	keV/s
Mean	energy	per	photon	detected	: 286.5792
Dose	Rate	(mGy/a)	-	>450	1.033566 5.31E-02
Dose	Rate	(mGy/a)	-	>1350	0.970686 4.59E-02
Dose	rate	(mGy/a)	-	energy	1.448787 7.27E-02

C.4. Cosmic dose rate

Sample Number SUERC	Field	Approx. Prescott & Stephan (1982) Parameters for Eqn. 1 ^a Read from Fig. 2				Approx. Altitude (km)	Surface Cosmic Dose Rate (Gy/ka)	Depth below surface (cm) ^b	Present Cosmic Dose Rate (Gy/ka) ^{c,d}	Approx. Representative Values (Est. from context and age)			
		Latitude N	F	J	H					Age (ka)	Depth below surface		Cosmic Dose Rate (Gy/ka) ^{c,d,e}
											Estimation	Estimated (cm)	
SUTL 2085	SI 1	61	0.24	0.77	4.10	0	0.293	40	0.23	0.9	.=present/2	20	0.25 ± 0.04
SUTL 2086	SI 2	61	0.24	0.77	4.10	0	0.293	55	0.21	0.9	.=present/2	28	0.24 ± 0.04
SUTL 2087	SI 3	61	0.24	0.77	4.10	0	0.293	65	0.21	0.8	.=present/2	32.5	0.23 ± 0.04
SUTL 2088	SI 4	61	0.24	0.77	4.10	0	0.293	73	0.20	0.6	.=present/2	36.5	0.23 ± 0.04
SUTL 2089	SI 5	61	0.24	0.77	4.10	0	0.293	85	0.20	0.9	.=present/2	42.5	0.22 ± 0.04

a. Cosmic dose rate as a fn. of altitude = $K*(F+J*exp(h/H))$: h = altitude (km) (Prescott & Stephan, 1982)

b. Depth values in normal text were quoted in fieldwork notes, those in italics were inferred from photos and notes

c. Sediment bulk density assumed = 1.6 g/cm³

d. Cosmic dose rate as a fn. of depth = $0.08*EXP(-0.02*(d*1.6))+0.21*EXP(-0.0007*(d*1.6))+0.00000008*(d*1.6)^2$: d = mass depth (g/cm²), parameters from fit to data in Prescott and Hutton (1988)

e. Estimated error = 5%Dcrep. + |Dcpresent-Dcrep.|

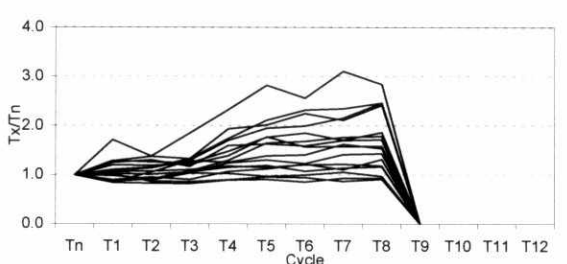
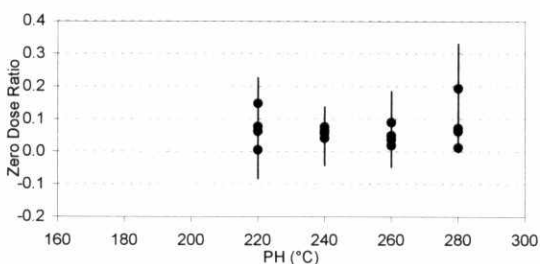
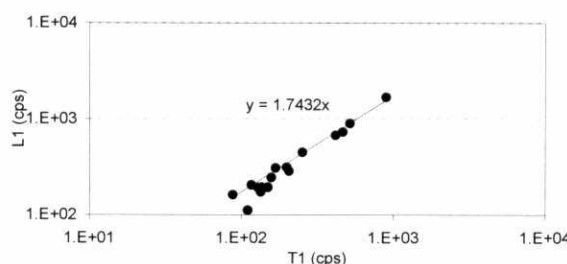
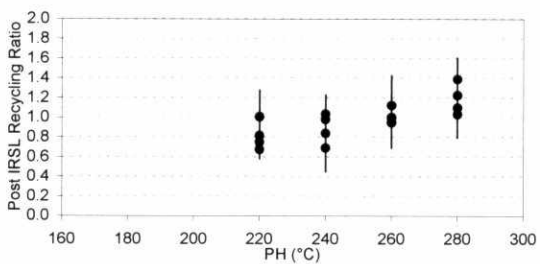
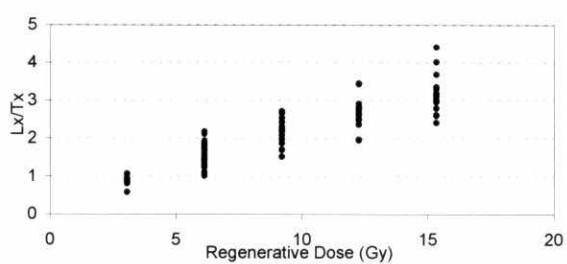
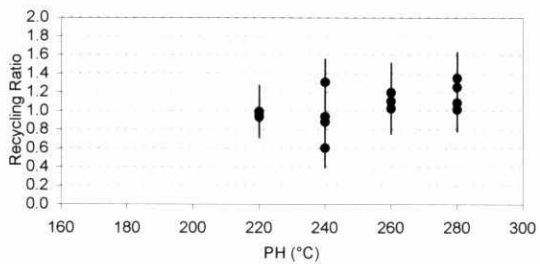
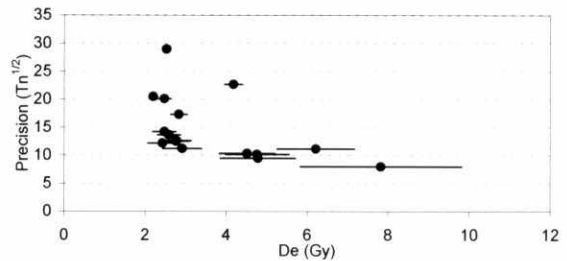
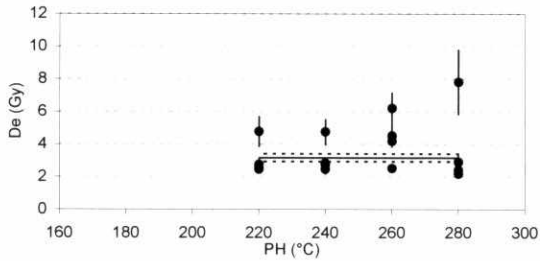
C.5. Water content

Sample Number SUERC	Field	Subsample for Water Content Determinations										Water Content as Mass Fraction			
		Sample From	"InSitu" date	Mass inc.T&G (g)	Sat. 2hr soak date	Mass inc.T&G (g)	DUL ON Drip date	Mass inc.T&G (g)	Dry date	Mass inc.T&G (g)	Tube + Gauze (g)	ISWC/ Dry Sed	SatWC/ Dry Sed	DULWC/ Dry Sed	Expected Burial (IS+DUL)/2
SUTL 2085	SI 1	all, in tube	211206	276.5	211206	290.2	221206	289.7	50107	259.5	155.2	0.16	0.29	0.29	0.23 ± 0.04
SUTL 2086	SI 2	all, in tube	211206	277.0	211206	289.9	221206	288.4	50107	258.3	154.6	0.18	0.30	0.29	0.24 ± 0.04
SUTL 2087	SI 3	all, in tube	211206	269.9	211206	285.6	221206	284.6	50107	253.5	153.3	0.16	0.32	0.31	0.24 ± 0.05
SUTL 2088	SI 4	all, in tube	211206	233.8	211206	245.0	221206	245.9	50107	222.7	160.5	0.18	0.36	0.37	0.28 ± 0.07
SUTL 2089	SI 5	all, in tube	211206	225.3	211206	243.1	221206	242.2	50107	215.7	154.2	0.16	0.45	0.43	0.29 ± 0.10

Appendix D. Equivalent dose determinations

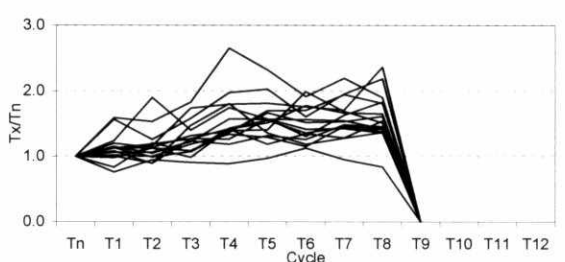
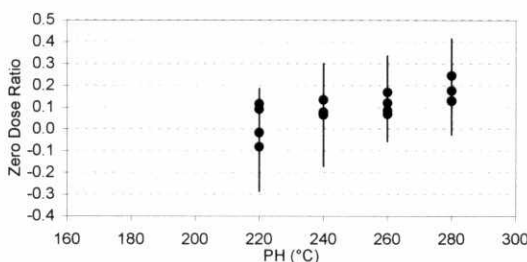
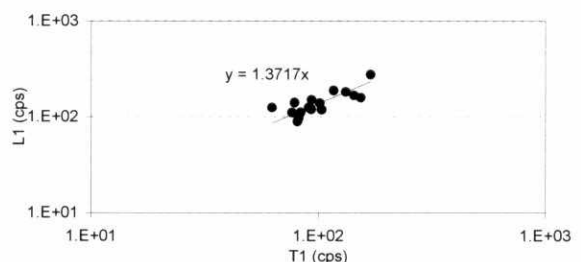
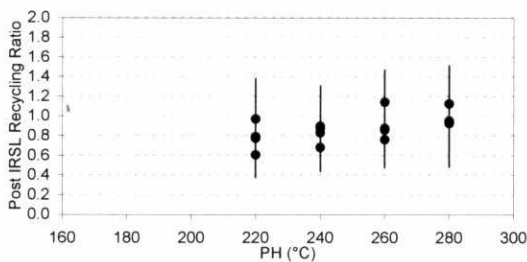
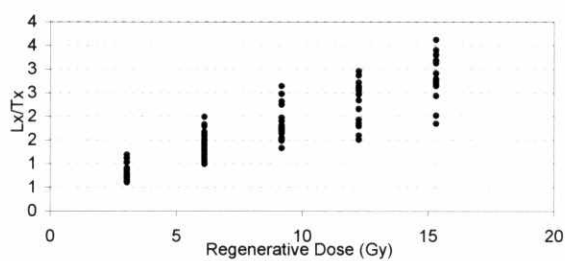
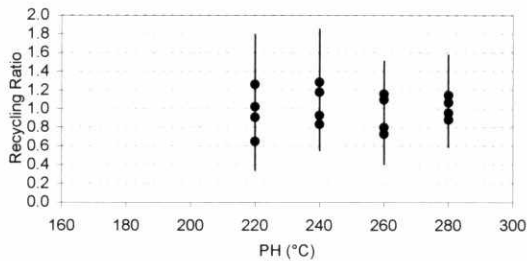
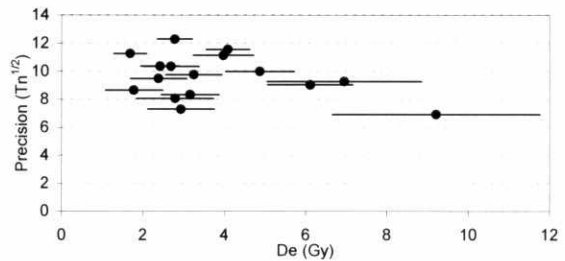
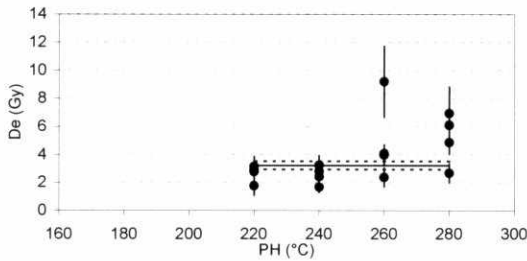
Sample SUTL 2085
 Date 300307 to 20407
 Reader Riso 1
 Source Calibration 0.1022 ± 0.0017 Gy/s
 Regenerative Dose Sequence (Gy)
 Dn D1 D2 D3 D4 D5 D6 D7 D8 D9
 0.00 6.12 3.06 9.19 12.25 15.32 -0.01 6.12 6.12 -0.01
 Test Dose (Gy) 3.06
 Measurement Signal Background
 OSL 60s@125°C, 240Ch 11-30 191-230
 IRSL 120s@50°C, 240Ch 11-30 191-230

Aliquot	Preheat (°C/30s)	Aliquot Mass (g)	Sensitivity (cps/ mg/Gy)	Dose Response Change (fm.)	D0 (Gy)	Err	Recycling Point		Post IRSL		Zero Dose		Equivalent Dose		AMC Robust Statistics V1.0	
							6.12 ratio	Gy error	6.12 ratio	Gy error	0.00 ratio	Gy error	(Gy)	error	Estimate	Estimate
17	220	2.8	18	1.1	18	8	0.98	0.25	1.01	0.27	0.006	0.089	2.760	0.327	Median	2.80056
18	220	4.2	32	1.2	43	22	0.93	0.12	0.67	0.10	0.078	0.043	2.473	0.164	A15 mean	2.96623 c=1.5: C
19	220	3.5	8	2.4	34	32	0.99	0.28	0.82	0.23	0.149	0.079	4.783	0.930	H15 mean	3.42792 c=1.5: C
20	220	3.3	19	1.3	19	8	0.94	0.21	0.75	0.16	0.063	0.057	2.586	0.286	MAD	0.35262
21	240	2.9	18	1.9	20	7	1.31	0.25	1.03	0.20	0.064	0.056	2.770	0.368	MADe	0.5228
22	240	3.1	11	1.6	32	34	0.60	0.21	0.69	0.24	0.042	0.084	4.763	0.787	sMAD	0.5228
23	240	2.7	36	1.0	12	3	0.94	0.15	0.84	0.14	0.057	0.047	2.831	0.204	H15 Std Dev	1.30703 c=1.5: C
24	240	3.5	19	1.4	28	15	0.88	0.17	0.98	0.19	0.076	0.062	2.473	0.286	LinCAM	3.166
25	260	2.3	119	1.2	104	51	1.03	0.07	1.00	0.07	0.020	0.011	2.525	0.072	seLinCAM	0.235
26	260	3.2	53	1.0	13	2	1.10	0.13	1.00	0.12	0.037	0.030	4.180	0.225	Sigma	0.813
27	260	4.0	10	1.8	19	9	1.20	0.32	1.12	0.30	0.090	0.096	6.214	0.961	seSigma	0.183
28	260	3.0	12	1.7	23	14	1.02	0.27	0.95	0.26	0.050	0.096	4.518	0.685		
29	280	3.3	15	1.8	24	11	1.01	0.24	1.03	0.24	0.072	0.056	2.422	0.358		
30	280	3.4	12	2.5	24	11	1.09	0.25	1.10	0.25	0.063	0.058	2.913	0.480		
31	280	2.6	53	2.5	34	7	1.35	0.12	1.39	0.12	0.013	0.014	2.198	0.112		
32	280	3.6	6	3.1	32	31	1.25	0.38	1.23	0.39	0.195	0.137	7.819	1.993		
Mean		3.2	28	1.7	30.0			1.04		0.98		0.067	Mean	3.639	Internal	n = 16
SD		0.5	29	0.6	21.6			0.18		0.19		0.048	SD	1.614	Error	LinCAM 3.166
SD/rtn		0.1	7	0.2	5.4			0.05		0.05		0.012	SD/rtn	0.404	0.174	Sigma 0.813
%err		4	26	9	18			4		5		18	%err	11		seLinCAM 0.235
																%err 7



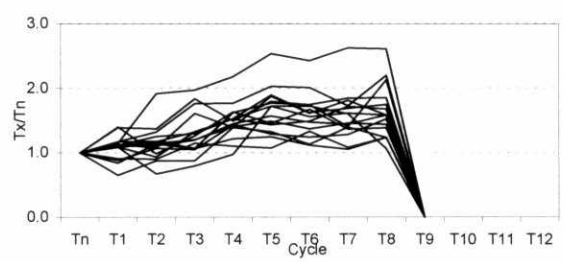
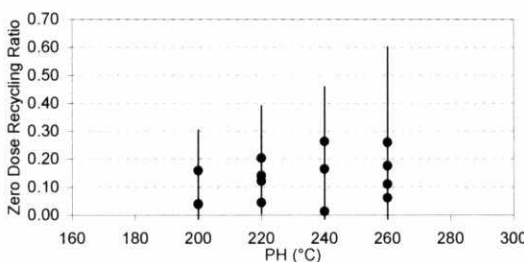
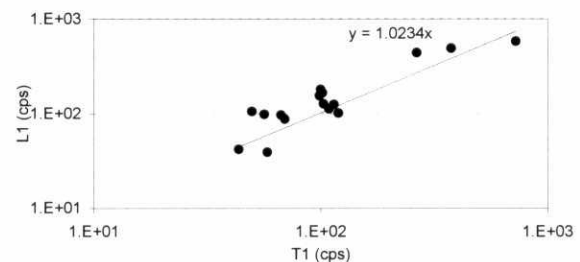
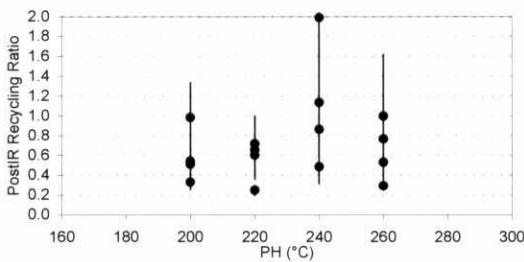
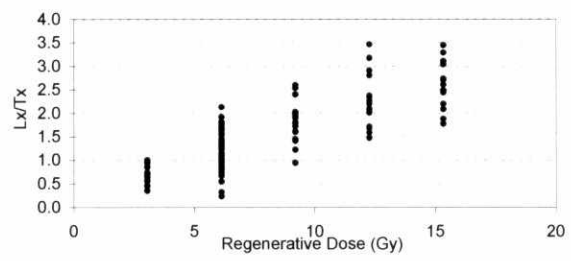
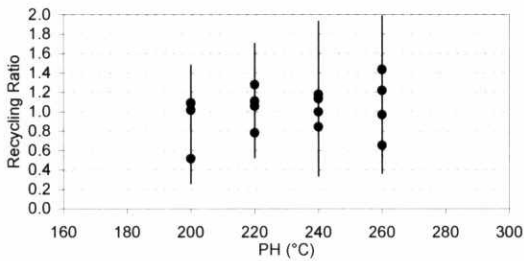
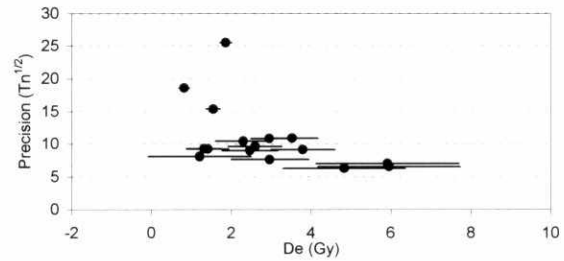
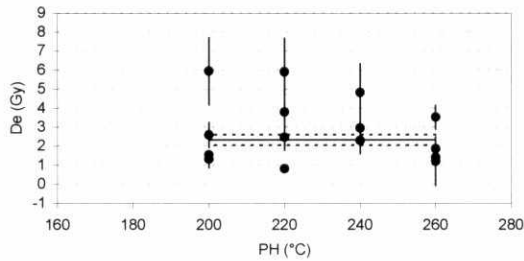
Sample SUTL 2086
 Date 300307 to 20407
 Reader Riso 1
 Source Calibration 0.1022 ± 0.0017 Gy/s
 Regenerative Dose Sequence (Gy)
 Dn D1 D2 D3 D4 D5 D6 D7 D8 D9
 0.00 6.12 3.06 9.19 12.25 15.32 -0.01 6.12 6.12 -0.01
 Test Dose (Gy) 3.06
 Measurement Signal Background
 OSL 60s@125°C, 240Cf 11-30 191-230
 IRSL 120s@50°C, 240Cl 11-30 191-230

Aliquot	Preheat (°C/30s)	Aliquot Mass (g)	Sensitivity (cps/ mg/Gy)	Change (fm.)	Dose Response		Recycling Point		Post IRSL		Zero Dose		Equivalent Dose		AMC Robust Statistics V1.0	
					D0 (Gy)	Err	6.12 ratio	Gy error	6.12 ratio	Gy error	0.00 ratio	Gy error	(Gy)	error	Estimate	Estimate
33	220	5.7	9	1.8	62	86.6	0.91	0.22	0.78	0.20	0.117	0.072	2.780	0.429	Median	3.04586
34	220	3.3	7	2.4	16	11.0	1.02	0.41	0.61	0.23	-0.015	-0.111	3.158	0.715	A15 mean	3.32557 c=1.5: C
35	220	4.2	6	2.0	10747	4E+06	0.65	0.31	0.79	0.38	0.092	0.090	1.778	0.705	H15 mean	3.5182 c=1.5: C
36	220	3.7	5	2.2	13	7.7	1.26	0.53	0.97	0.41	-0.081	-0.205	2.933	0.818	MAD	0.79724
37	240	4.9	6	1.9	39	47.7	0.83	0.28	0.68	0.24	0.135	0.107	3.250	0.695	MADe	1.18199
38	240	4.7	9	1.6	44	50.6	1.18	0.33	0.88	0.27	0.079	0.122	1.686	0.409	sMAD	1.18199
39	240	4.4	8	1.6	14	6.4	0.93	0.29	0.83	0.27	0.068	0.099	2.422	0.480	H15 Std Dev	1.59093 c=1.5: C
40	240	3.9	5	1.9	115	581.2	1.29	0.57	0.90	0.41	0.066	0.237	2.790	0.951	LinCAM	3.227
41	260	3.7	4	2.7	250	2914.7	0.73	0.32	0.88	0.40	0.169	0.169	9.209	2.555	seLinCAM	0.292
42	260	5.0	8	1.6	8	2.7	0.80	0.24	0.76	0.24	0.069	0.094	3.976	0.746	Sigma	0.874
43	260	3.9	8	1.8	6	2.4	1.10	0.41	0.86	0.33	0.120	0.154	2.381	0.695	seSigma	0.261
44	260	4.8	9	1.5	9976	3E+06	1.16	0.33	1.14	0.33	0.086	0.143	4.088	0.542		
45	280	4.4	6	1.7	10	4.8	0.96	0.37	0.93	0.35	0.131	0.156	6.950	1.901		
46	280	3.7	7	1.5	2946	340820	1.14	0.43	1.13	0.39	0.177	0.152	6.112	1.053		
47	280	4.7	7	1.1	11223	5E+06	1.07	0.46	0.93	0.44	0.245	0.171	2.688	0.685		
48	280	4.5	7	1.5	66	151.5	0.88	0.29	0.95	0.32	0.129	0.137	4.875	0.848		
Mean		4.3	7	1.8	2220.9			0.99	0.88		0.099	Mean	3.818	Internal		n = 16
SD		0.6	1	0.4	4249.0			0.19	0.14		0.075	SD	2.050	Error		LinCAM 3.227
SD/rtN		0.2	0	0.1	1062.2			0.05	0.04		0.019	SD/rtN	0.512	0.261		Sigma 0.874
%err		4	5	5	48			5	4		19	%err	13			seLinCAM 0.292
																%err 9



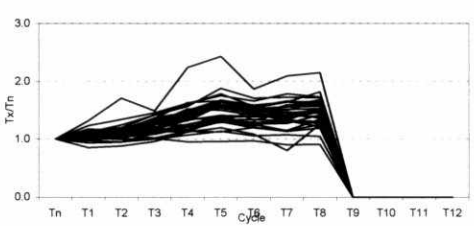
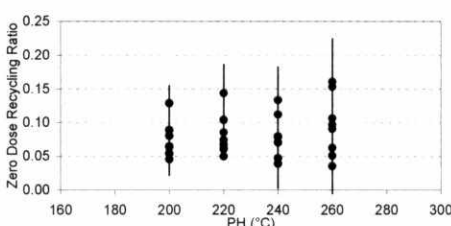
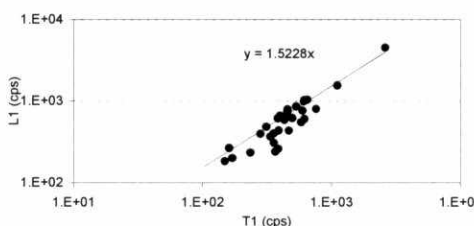
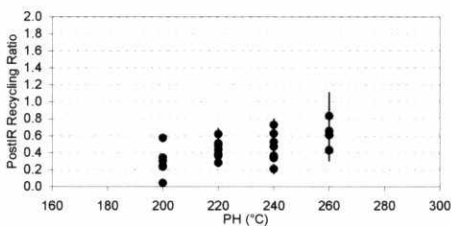
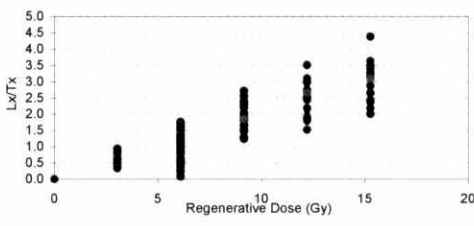
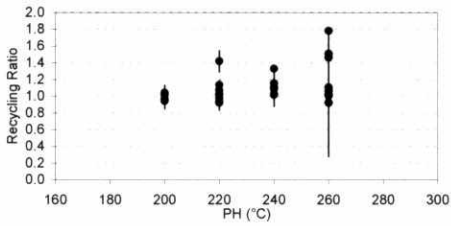
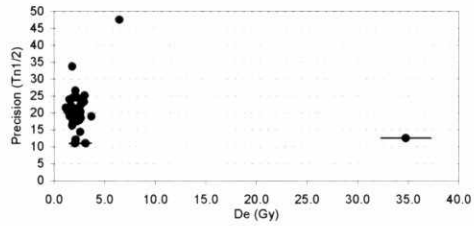
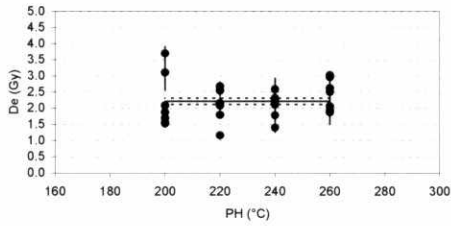
Sample SUTL 2087
 Date 250307 to 260307
 Reader Riso 1
 Source Calibration 0.1023 ± 0.0017 Gy/s
 Regenerative Dose Sequence (Gy)
 Dn D1 D2 D3 D4 D5 D6 D7 D8 D9
 0.00 6.12 3.06 9.19 12.26 15.33 -0.01 6.12 6.12 0.00
 Test Dose (Gy) 3.06
 Measurement Signal Background
 OSL 60s@125°C, 240C† 11-30 191-230
 IRSL 120s@50°C, 240C† 11-30 191-230

Aliquot	Preheat (°C/30s)	Aliquot Mass (g)	Sensitivity (cps/mg/Gy)	Dose Response (D0 (Gy) Err)	Recycling Point (6.12 Gy ratio error)	Post IRSL (6.12 Gy ratio error)	Zero Dose (0.00 Gy ratio error)	Equivalent Dose (Gy) error	AMC Robust Statistics V1.0	
									Estimate	Estimate parameter
2	200	5.0	6	1.6 64 136	1.09 0.39	0.99 0.35	0.160 0.146	2.597 0.675	Median	2.53077
3	200	4.6	17	1.9 29 10	1.02 0.16	0.33 0.06	0.039 0.041	1.544 0.174	A15 mean	2.70994 c=1.5: C
4	200	2.8	5	2.6 28 31	0.52 0.26	0.51 0.26	-0.011 -0.091	5.951 1.779	H15 mean	2.72459 c=1.5: C
5	200	3.2	9	2.2 20 12	1.09 0.35	0.54 0.17	0.040 0.081	1.319 0.450	MAD	1.05832
6	220	3.3	34	1.5 52 28	1.06 0.13	0.25 0.05	0.045 0.039	0.818 0.133	MADe	1.56907
7	220	2.1	8	2.1 42 89	1.11 0.54	0.66 0.30	0.205 0.189	5.910 1.789	sMAD	1.56907
8	220	3.1	9	1.7 5980 1E+06	1.28 0.43	0.72 0.28	0.142 0.136	2.464 0.695	H15 Std Dev	1.56855 c=1.5: C
9	220	3.9	7	1.9 64 127	0.78 0.26	0.61 0.21	0.122 0.105	3.794 0.798	LinCAM	2.328
10	240	2.9	5	1.7 43 98	1.14 0.80	1.99 1.53	-0.036 -0.268	4.826 1.524	seLinCAM	0.276
11	240	2.9	7	1.9 103 400	1.00 0.40	1.14 0.47	0.166 0.150	2.965 0.971	Sigma	0.853
12	240	3.9	10	1.2 11 4	0.84 0.29	0.49 0.17	0.014 0.090	2.955 0.460	seSigma	0.232
13	240	3.5	10	1.7 10481 4E+06	1.18 0.40	0.87 0.32	0.264 0.197	2.301 0.706		
14	260	3.9	7	1.4 6 2	0.65 0.29	0.53 0.26	0.111 0.121	1.411 0.521		
15	260	2.6	8	1.5 8673 4E+06	1.22 0.77	1.00 0.62	0.261 0.343	1.207 1.288		
16	260	3.8	10	1.3 88 264	0.97 0.35	0.77 0.27	0.062 0.124	3.528 0.644		
17	260	4.8	44	1.7 19451 2E+06	1.44 0.13	0.29 0.04	0.178 0.037	1.861 0.143		
Mean		3.5	12	1.7 2820.9	1.02	0.73	0.110	Mean 2.841 Internal		n = 16
SD		0.8	11	0.4 5608.7	0.23	0.42	0.092	SD 1.606 Error		LinCAM 2.328
SD/rtN		0.2	3	0.1 1402.2	0.06	0.11	0.023	SD/rtN 0.402 0.238		Sigma 0.853
%err		6	23	5 50	6	15	21	%err 14		seLinCAM 0.276
										%err 12



Sample SUTL 2088
 Date 110507 to 130507
 Reader Riso 1
 Source Calibration 0.1019 ± 0.0017 Gy/s
 Regenerative Dose Sequence (Gy)
 Dn D1 D2 D3 D4 D5 D6 D7 D8 D9
 0.00 6.10 3.05 9.16 12.22 15.28 -0.01 6.10 6.10 0.00
 Test Dose (Gy) 3.05
 Measurement Signal Background
 OSL 60s@125°C, 240C 11-30 191-230
 IRSL 120s@50°C, 240C 11-30 191-230

Aliquot	Preheat (°C/30s)	Aliquot Mass (g)	Sensitivity (cps/mg/Gy)	Dose Response		Recycling Point		Post IRSL		Zero Dose		Equivalent Dose		AMC Robust Statistics V1.0		
				D0 (Gy)	Err	6.10 Gy	ratio error	6.10 Gy	ratio error	0.00 Gy	ratio error	(Gy)	error	Estimate	Estimate parameter	
2	200	4.3	37	1.4	41	17	1.04	0.12	0.24	0.04	0.065	0.034	1.697	0.133		
3	200	4.6	41	1.6	33	10	0.96	0.10	0.35	0.05	0.089	0.032	1.533	0.112	Median 2.21306	
4	200	4.5	26	1.7	37	15	0.95	0.12	0.24	0.05	0.046	0.033	1.564	0.143	A15 mean 2.27503 c=1.5: C	
5	200	5.4	25	1.9	36	11	0.96	0.10	0.30	0.04	0.055	0.027	2.085	0.133	H15 mean 2.28685 c=1.5: C	
6	220	3.2	31	1.4	42	22	0.93	0.13	0.39	0.07	0.050	0.043	2.157	0.184	MAD 0.39129	
7	220	4.1	41	1.7	97	75	1.14	0.11	0.28	0.04	0.068	0.034	2.678	0.143	MADe 0.58013	
8	220	4.2	35	1.5	34	11	0.98	0.11	0.51	0.06	0.062	0.029	2.085	0.133	sMAD 0.58013	
9	220	4.2	29	1.6	77	59	1.03	0.12	0.36	0.05	0.061	0.034	2.545	0.164	H15 Std Dev 0.60934 c=1.5: C	
10	240	3.7	27	1.8	78	71	1.11	0.15	0.34	0.06	0.047	0.049	2.320	0.204		
11	240	2.4	57	1.7	6	0	1.33	0.15	0.36	0.06	0.079	0.041	1.400	0.143	LinCAM 2.213	
12	240	3.9	51	1.3	9639	767273	1.02	0.11	0.34	0.05	0.080	0.040	2.269	0.143	seLinCAM 0.101	
13	240	4.0	33	1.6	37	14	1.11	0.13	0.53	0.07	0.071	0.037	2.320	0.164	Sigma 0.512	
14	260	4.4	40	1.3	3329	109000	0.92	0.11	0.43	0.07	0.063	0.045	2.964	0.184	seSigma 0.076	
15	260	3.9	10	1.3	75	193	1.78	0.73	0.66	0.28	0.153	0.189	2.065	0.562		
16	260	5.8	19	1.3	29	11	1.11	0.16	0.65	0.11	0.051	0.053	2.627	0.215		
17	260	4.1	30	1.3	10612	1439435	1.51	0.23	0.61	0.12	0.106	0.079	1.942	0.215		
2	200	4.3	28	1.6	44	21	0.97	0.12	0.31	0.05	0.064	0.036	3.700	0.214		
3	200	4.6	43	1.6	34	10	1.03	0.10	0.24	0.04	0.054	0.026	1.876	0.112		
4	200	4.5	165	1.8	7311	150885	1.02	0.04	0.05	0.01	0.080	0.009	6.452	0.092		
5	200	5.4	7	2.4	28	16	1.01	0.23	0.58	0.14	0.129	0.074	3.109	0.550		
6	220	3.2	16	1.4	3539	252698	1.42	0.34	0.62	0.17	0.144	0.097	34.769	2.487		
7	220	4.1	91	1.1	44	16	1.02	0.09	0.38	0.05	0.085	0.031	1.794	0.092		
8	220	4.2	29	1.3	131	215	0.94	0.13	0.49	0.07	0.074	0.044	2.558	0.163		
9	220	4.2	36	1.7	9743	899248	1.07	0.12	0.44	0.06	0.104	0.041	1.162	0.112		
10	240	3.7	18	1.6	4089	283446	1.09	0.21	0.63	0.14	0.133	0.085	2.589	0.347		
11	240	2.4	20	1.5	91	165	1.03	0.24	0.47	0.13	0.047	0.088	2.130	0.316		
12	240	3.9	60	1.6	4678	163639	1.09	0.10	0.21	0.04	0.112	0.034	2.110	0.122		
13	240	4.0	22	1.7	31	12	1.16	0.17	0.73	0.11	0.039	0.044	1.784	0.204		
14	260	4.4	24	1.5	11438	1691598	1.02	0.15	0.66	0.12	0.091	0.062	2.508	0.255		
15	260	3.9	54	1.0	37	10	1.01	0.09	0.83	0.08	0.036	0.021	3.027	0.112		
16	260	5.8	17	1.8	17277	3594000	1.46	0.22	0.43	0.10	0.161	0.077	1.876	0.265		
17	260	4.1	33	1.3	34	15	1.06	0.15	0.43	0.08	0.097	0.051	2.620	0.214		
Mean		4.2	37	1.5	2586		1.10		0.44		0.081	Mean	3.385	Internal	n = 30	
SD		0.8	29	0.3	4513		0.19		0.17		0.034	SD	5.800	Error	LinCAM 2.213	
SD/rtn		0.1	5	0.0	798		0.03		0.03		0.006	SD/rtn	1.025	0.083	Sigma 0.512	
%err		3	13	3	31		3		7		7	%err	30		seLinCAM 0.101	
															%err	5



Sample SUTL 2089
 Date 300307 to 20407
 Reader Riso 1
 Source Calibration 0.1022 ± 0.0017 Gy/s
 Regenerative Dose Sequence (Gy)
 Dn D1 D2 D3 D4 D5 D6 D7 D8 D9
 0.00 6.12 3.06 9.19 12.25 15.32 -0.01 6.12 6.12 -0.01
 Test Dose (Gy) 3.06
 Measurement Signal Background
 OSL 60s@125°C, 240C† 11-30 191-230
 IRSL 120s@50°C, 240C† 11-30 191-230

Aliquot	Preheat (°C/30s)	Aliquot Mass (g)	Sensitivity (cps/mg/Gy)	Dose Response		Recycling Point		Post IRSL		Zero Dose		Equivalent Dose		AMC Robust Statistics V1.0			
				D0 (Gy)	Err	6.12 Gy ratio	error	6.12 Gy ratio	error	0.00 Gy ratio	error	(Gy)	error	Estimate	Estimate Parameter		
1	220	4.5	10	1.7	145	489	0.85	0.22	0.58	0.16	0.098	0.082	2.034	0.409	Median	3.3065	
2	220	4.8	7	2.4	71	120	1.26	0.33	0.76	0.21	0.029	0.107	2.801	0.491	A15 mean	3.30249 c=1.5: C	
3	220	5.7	4	2.5	12	6	1.11	0.38	0.83	0.28	0.166	0.152	3.680	1.032	H15 mean	3.34438 c=1.5: C	
4	220	4.1	9	1.8	65	97	0.82	0.23	0.64	0.18	0.051	0.068	3.720	0.521	MAD	0.45995	
5	240	4.6	29	2.3	12691	1E+06	1.43	0.14	0.32	0.05	0.059	0.031	1.922	0.143	MADe	0.68192	
6	240	4.4	8	1.7	77	211	0.83	0.28	0.90	0.30	0.210	0.134	3.352	0.787	sMAD	0.68192	
7	240	4.2	13	2.1	22	9	1.15	0.22	0.91	0.17	0.064	0.060	3.240	0.399	H15 Std De	1.0288 c=1.5: C	
8	240	3.5	13	1.7	72	117	1.05	0.27	0.74	0.21	0.056	0.121	3.261	0.531	LinCAM	3.095	
9	260	3.0	7	1.7	13936	8E+06	1.33	0.56	1.05	0.46	0.186	0.249	4.794	1.175	seLinCAM	0.220	
10	260	3.9	8	1.5	12	7	0.99	0.36	0.91	0.35	0.218	0.157	4.681	1.022	Sigma	0.646	
11	260	3.9	10	1.4	623	14861	1.20	0.40	0.92	0.29	0.261	0.188	5.223	1.002	seSigma	0.195	
12	260	3.3	6	2.3	17	11	0.91	0.37	0.85	0.37	0.190	0.143	3.516	1.155			
13	280	3.8	22	1.8	58	50	1.64	0.28	1.06	0.20	0.143	0.092	2.218	0.327			
14	280	4.1	10	1.6	10	3	1.01	0.27	0.95	0.27	0.061	0.099	3.066	0.480			
15	280	2.9	23	2.7	138	178	1.12	0.16	1.11	0.15	0.006	0.026	3.700	0.276			
16	280	3.9	7	1.7	31	37	0.64	0.26	0.73	0.31	0.113	0.124	2.688	0.818			
Mean		4.0	12	1.9	1748.7		1.08		0.83		0.119	Mean	3.368	Internal	n = 16	LinCAM	3.095
SD		0.7	7	0.4	4522.5		0.25		0.20		0.078	SD	0.954	Error		Sigma	0.646
SD/rTN		0.2	2	0.1	1130.6		0.06		0.05		0.019	SD/rTN	0.238	0.184		seLinCAM	0.220
%err		4	15	5	65		6		6		16	%err	7			%err	7

